AFGL-TR-81-0218
ENVIRONMENTAL RESEARCH PAPERS, NO. 750

LEVEL II

12

Short-Range Forecasting of Cloudiness and Precipitation Through Extrapolation of GOES Imagery

H. STUART MUENCH

16 July 1981

METEOROLOGY DIVISION PROJECT 6670
AIR FORCE GEOPHYSICS LABORATORY
HANSCOM AFB, MASSACHUSETTS 01731

AIR FORCE SYSTEMS COMMAND, USAF

This report has been reviewed by the ESD Information Office (OI) and is releasable to the National Technical Information Service (NTIS).

This technical report has been reviewed and is approved for publication.

FOR THE COMMANDER

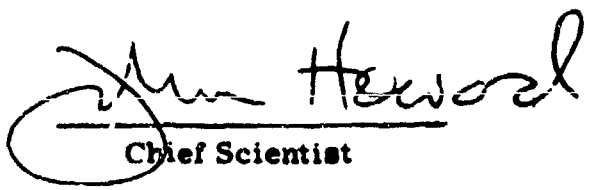

Chief Scientist

Qualified requestors may obtain additional copies from the Defense Technical Information Center. All others should apply to the National Technical Information Service.

Unclassified

SECURITY CLASSIFICATION OF THIS PAGE (When Data Entered)

REPORT DOCUMENTATION PAGE	READ INSTRUCTIONS BEFORE COMPLETING FORM
1. REPORT NUMBER: AFGL-TR-81-0218	2. GOVT ACCESSION NO.: AD-A108678
3. RECIPIENT'S CATALOG NUMBER	
4. TITLE (and Subtitle): SHORT-RANGE FORECASTING OF CLOUDINESS AND PRECIPITATION THROUGH EXTRAPOLATION OF GOES IMAGERY	5. TYPE OF REPORT & PERIOD COVERED: Scientific. Final.
	6. PERFORMING ORG. REPORT NUMBER: ERP No. 750
7. AUTHOR(s): H. Stuart Muench	8. CONTRACT OR GRANT NUMBER(s)
9. PERFORMING ORGANIZATION NAME AND ADDRESS: Air Force Geophysics Laboratory (LYP), Hanscom AFB, Massachusetts 01731	10. PROGRAM ELEMENT, PROJECT, TASK AREA & WORK UNIT NUMBERS: 62101F, 66700804
11. CONTROLLING OFFICE NAME AND ADDRESS: Air Force Geophysics Laboratory (LYP), Hanscom AFB, Massachusetts 01731	12. REPORT DATE: 16 July 1981
	13. NUMBER OF PAGES: 46
14. MONITORING AGENCY NAME & ADDRESS(if different from Controlling Office)	15. SECURITY CLASS. (of this report): Unclassified
	15a. DECLASSIFICATION/DOWNGRADING SCHEDULE

16. DISTRIBUTION STATEMENT (of this Report)

Approved for public release; distribution unlimited.

17. DISTRIBUTION STATEMENT (of the abstract entered in Block 20, if different from Report)

18. SUPPLEMENTARY NOTES

19. KEY WORDS (Continue on reverse side if necessary and identify by block number)

Satellite meteorology
Meteorology
GOES
Objective forecasting
Precipitation forecasting
Cloud forecasting
Short-range forecasting

20. ABSTRACT (Continue on reverse side if necessary and identify by block number)

This report describes the development and testing of an objective technique to forecast cloudiness and precipitation through extrapolation of satellite imagery. By ~~utilizing~~ an objectively determined cloud-motion vector, the technique makes local forecasts of satellite parameters (brightness and IR temperature), with high temporal resolution, using simple linear extrapolation. Algorithms are then used to convert the satellite parameters to total cloud cover, probability of 1-hour precipitation, and presence of low, middle, and high clouds. The test program computed motion vectors and

DD FORM 1 JAN 73 1473 EDITION OF 1 NOV 65 IS OBSOLETE

Unclassified

SECURITY CLASSIFICATION OF THIS PAGE (When Data Entered)

made forecasts out to 7 hours, in half-hour steps, at 30 locations. The program was tested on 12 spring and fall cases, using half-hourly GOES imagery. For periods beyond 2 hours, forecasts of cloud cover and precipitation were markedly better than persistence, while deficiencies in specification hindered short-period performance. Forecasts of cloud layers were worse than persistence due to inadequate specification algorithms. The net results were quite encouraging, and further refinements and developments are planned.

Contents

Illustrations

Illustrations

Tables

Short-Range Forecasting of Cloudiness and Precipitation Through Extrapolation of GOES Imagery

1. INTRODUCTION

An admitted deficiency in meteorology is the limited ability to forecast sudden changes in weather conditions. In the past, forecasters blamed the combination of small-scale complexities in the weather patterns, and the large spacing in the observing network. Now, with the high resolution of satellite imagery data as well as ground-based radar data, this excuse is no longer valid, and there are ample opportunities to develop short-range prediction techniques.

An effort has been underway at Air Force Geophysics Laboratory (AFGL) to utilize satellite information in short-range forecasting. The first objective technique to be explored is that of simple extrapolation, in which the basic weather patterns are assumed to move, unchanged, in a simple straight line. To make a forecast, one requires a means to determine the motion vector, a procedure to use the motion vector to forecast satellite imagery parameters, and algorithms to convert the imagery parameters to surface weather conditions. This report will describe a test of the extrapolation concept, operating in an automated mode. The first step is the construction of a forecast model. Next is the compilation of satellite and weather data, followed by computer execution of the forecast model. Finally, there is the presentation of verification scores and a discussion of the results.

Received for Publication 14 July 1981

2. EXTRAPOLATION TECHNIQUES

Simple extrapolation of weather patterns has been an important forecast technique for over 100 years. To make forecasts of large areas, one uses a series of weather charts, often 12 hours apart, and notes the motion of significant features such as fronts, pressure centers, "thickness" contours, or jet streams. The forecaster then extrapolates the positions of these features 12, 24, or 36 hours into the future, and draws up a "prognostic" weather chart. For many years, weather centrals have been preparing and disseminating prognostic charts with 12-hour time intervals out to about 48 hours. While these charts are convenient for viewing the "whole picture," the coarse temporal resolution requires that the forecaster must make careful temporal and spatial interpolations for local operational forecasts.

The extrapolation techniques can also be applied to a specific location to produce local forecasts of high temporal resolutions. An example of such a scheme applied to satellite imagery is shown schematically in Figure 1. From a sequence of satellite images (visual or IR digital data), a motion vector is determined by comparing the positions of features. Next, the motion vector is reversed in direction and one marches "upstream," converting distance in the image to time, by using the speed of the motion vector. For example, if the pattern is moving at 15 mps (30 kts) the condition to expect in one hour exists now 54 km (30NM) in the upstream direction. One then makes forecasts of satellite-measured parameters (visible or IR brightness) at, say, half-hour intervals as far out into the future as one might expect both the pattern and motion to remain unchanged. The final step is to convert the forecast satellite parameters to surface weather conditions, and one then has a detailed short-range forecast.

3. TEST FORECAST MODEL

3.1 Model Structure

The basic extrapolation principle is used currently in an AWS operational cloud forecast model[1] and also in a McGill University precipitation model[2]:

*Computer models have replaced the synoptic meteorologists at these centrals, but the output prognostic charts are similar.

1. Tarbell, T. C. and Hoke, J. E. (1980) The automated analysis/forecast model system at the Air Force Global Weather Central, Proc. AMS Eighth Conference on Weather Forecasting and Analysis, pp. 262-269.
2. Bellon, A. and Austin, G. L. (1978) The evaluation of two years of real-time operation of a short-term precipitation forecasting procedure (SHARP). J. Appl. Meteor., 17:1778-1787.

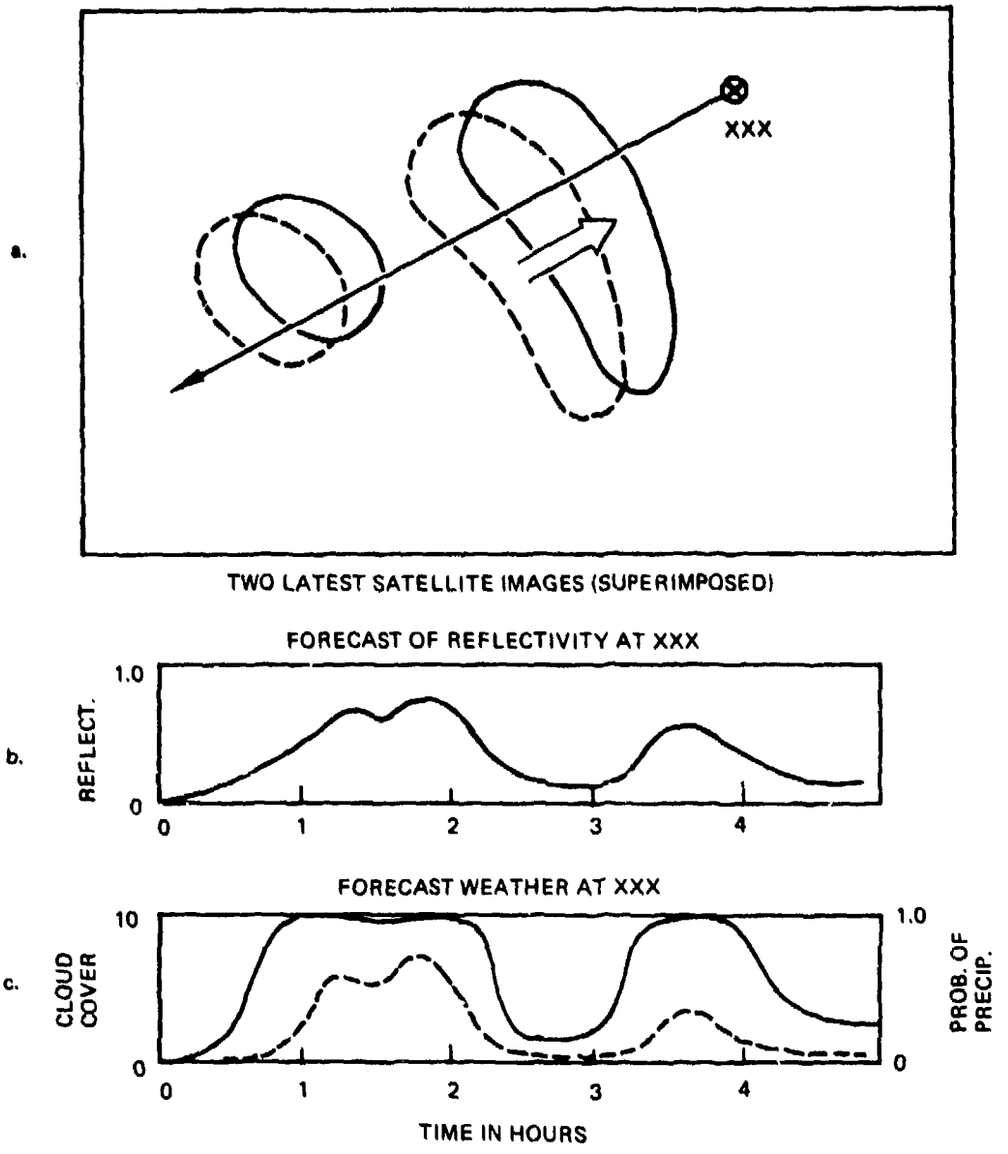

Figure 1. Illustration of Forecasting Through Extrapolation of Satellite Imagery. (a) Derive motion vector, (b) Predict reflectivity by looking "upstream," and (c) Convert forecast reflectivity to surface weather

While these operational models were not designed to produce local forecasts with high temporal resolution, they each contain some of the features illustrated in Figure 1, and provided a basis for this test forecast model. As can be seen in Figure 1, there are three separate steps leading to the production of the local weather forecast. The first step consists of determining the speed and direction of cloud-system motion. Next, the satellite image is used to produce a series of forecast satellite parameters. Finally, the satellite parameters are converted pertinent weather variables.

3.2 Motion Vectors

Several groups have developed computer-based techniques to derive motion vectors from sequences of satellite images[3,4]. The principal application of these techniques, however, has been to estimate upper-level winds in data-sparse regions. In the reports by Muench and Hawkins,[5] and Muench,[6] several candidate techniques were evaluated for their suitability for use in an automated short-range forecast model based on extrapolation. These techniques included a "cloud-tracking" technique, a fast-Fournier-transform cross-covariance technique, and a binary cross-covariance technique. In addition, winds aloft at 700 and 500 mb were tested as possible motion vectors.

All of the basic techniques worked well when the cloud patterns were near the center of the working arrays. Only the binary cross-covariance technique, however, worked equally as well when the cloud patterns were predominately near the edges of the arrays. In an interactive application, an operator could center the array manually over a cloud pattern, but such positioning would not be simple in an automatic mode. Another result was that either a recent 700-mb wind or one-half the 500-mb wind produces forecasts nearly as good as those produced by covariance derived motion vector and, in many instances, the upper-level winds can be obtained more easily. In view of these results, the binary

---

3. Leese, J. A. and Novak, C. S. (1971) An automated technique for obtaining cloud motion from geosynchronous satellite data using cross-correlation. J. Appl. Meteor., 10:118-132.

4. Wolfe, D. E., Hall, D. J., and Endlich, R. M. (1977) Experiments in automatic cloud tracking using SMS-GOES data, J. Appl. Meteor., 16:1219-1230.

5. Muench, H. S. and Hawkins, R. S. (1979) Short-Range Forecasting Through Extrapolation of Satellite Imagery Patterns, AFGL-TR-79-0096, ADA073081.

6. Muench, H. S. (1979) Short-Range Forecasting Through Extrapolation of Satellite Imagery Patterns Part II, Testing Motion Vector Techniques, AFGL-TR-79-0294, ADA 086862.

cross-covariance and the 700-mb wind techniques were chosen in this test to forecast surface weather conditions using satellite data.

Objective forecast techniques using extrapolation have been developed for weather radar data bases, both experimentally[7,8] and operationally.[2] A common problem is that successive pairs of images often yield motion vectors that oscillate in time, and one would expect that a more stable motion vector would produce more reliable forecasts. An obvious solution is to perform a time-average on a series of motion vectors, and for this test, a "running-time" average was adopted. At each time step, the average was updated by adding 30% of the latest motion vector to 70% of the old average motion vector. When a test case is started, there is no old average motion vector, so the first average motion vector was 50% of the 700-mb wind and 50% of the first motion vector. Table 1 shows the contribution of each computed motion vector to the time average at different time steps after the case was started.

Table 1. Contribution of Computed Vectors to Running Time Average

Step	Time	700-mb	1	2	3	4	5	6	7
1	.5	.500	.500	-	-	-	-	-	-
2	1.0	.350	.350	.300	-	-	-	-	-
3	1.5	.245	.245	.210	.300	-	-	-	-
4	2.0	.172	.172	.147	.210	.300	-	-	-
5	2.5	.120	.120	.103	.147	.210	.300	-	-
6	3.0	.084	.084	.072	.103	.147	.210	.300	-
7	3.5	.059	.059	.050	.072	.103	.147	.210	-

3.3 Forecasting Satellite Parameters

Once having established a motion vector, a procedure can be programmed easily to reverse the vector and look upstream in an array of either visible or IR data to determine what values will arrive at which time. A previous test[6] indicated that skill relative to persistence was small, but increasing with time out to 3 hours. For this follow-on test, the forecast time was extended to 7 hours. To assure temporal resolution, half-hourly time steps were chosen, even though

7. Muench, H. S. and Lamkin, W. E. (1976) The Use of Digital Radar in Short-Range Forecasting, AFGL-TR-76-0173, ADA033624.

8. Browning, K. A. (1980) Radar as part of an integrated system for measuring and forecasting rain in the UK: progress and plans, Weather, 35, pp. 94-104.

this meant that only half of the forecasts could be verified by the airways observations taken "on-the-hour." If one is to make a forecast for the I^{th} half-hour time period, he would look upstream a distance z defined by

$$Z = c \cdot s \cdot I$$

where c is the speed of the motion vector, and s is the scale factor that converts to units of grid distance.

Of course it would be very unlikely that the point at the distance z upstream would be found to lie exactly on top of a gridpoint of satellite data, and some interpolation would be necessary using data from surrounding gridpoints. Also, we must recognize that there are uncertainties in both the direction of the vector and the speed. To allow for these uncertainties, we should include more of the surrounding gridpoints in the interpolation, particularly for the longer time intervals. (Large value of I.) In this model, a 9 x 9 array of gridpoints was used, surrounding the upstream point at the time interval I. At each of the 81 points, a weighting function was computed, based on the distance from the upstream point (near the center of the 9 x 9 array), as well as the time interval. If the distance from the gridpoint i, j to the upstream point is $p_{i,j}$ then the weighting function $W_{i,j}$ is computed by

$$W_{i,j} = \gamma / (\gamma + p_{i,j}^2)$$

$$\gamma = (0.4 + c \cdot s) \cdot I + 0.10 \quad .$$

This formula compensates for errors of about 20% in speed and 15° in direction. Characteristics of the weighting function can be seen in more detail in Figure 2. The weighting function approaches 1.0 at long time intervals, and puts nearly all the weight on the four nearest points for the shortest time intervals. To compute a forecast of a satellite parameter, for example, the visible reflectivity R_f, then

$$R_f = \frac{\sum_{i=1}^{9} \sum_{j=1}^{9} R_{i,j} W_{i,j}}{\sum_{i=1}^{9} \sum_{j=1}^{9} W_{i,j}} \quad .$$

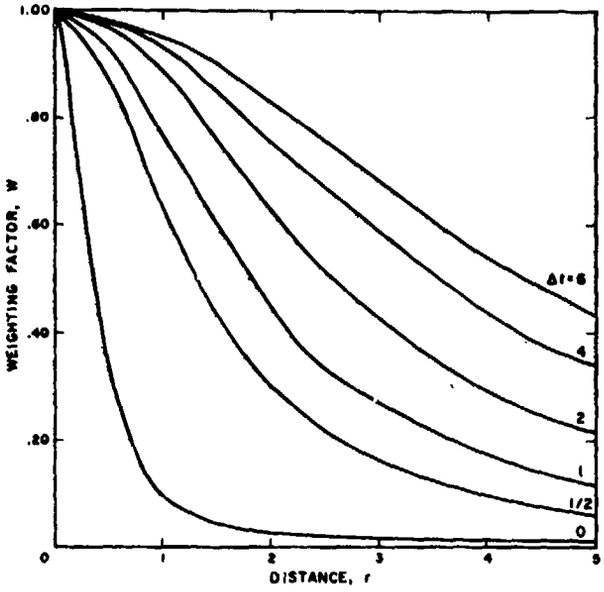

Figure 2. Weighting Function for Points in 9 x 9 Array Surrounding "Upstream" Point, as a Function of Forecast Time and Distance

3.4 Conversion to Surface Weather

Given forecasts of visible reflectivity and IR emission, one needs algorithms to convert these forecast parameters to their equivalent surface weather conditions. In choosing the weather elements to forecast there were three important considerations:

i. Which elements are most directly related to reflectivity and IR emission?
ii. Which elements are of greatest importance to airfield operations?
iii. Which elements can be most readily verified by observations?

The first element to be chosen was cloud amount. To determine cloud amount from satellite digital data, a natural approach would be to start with an array of data similar in size to the area seen by a ground observer -- roughly a 20-km diameter circle. Then one would use the finest resolution data available and simply count the number of "bright" values, and divide the total by all values to get the cloud coverage. There are two problems with this approach. First, clouds have resolution much smaller than the finest satellite resolution routinely

available. A "bright" value of even half-mile resolution data might be made up of some clear sky and some "very bright" clouds, or it might be uniformly "bright" clouds -- there is no obvious way to tell. Second, there is a continuous spectrum of sky reflectivities (and IR emissions) from dark, clear skies, to light haze, to thin clouds, all the way to bright, dense clouds. There is no physically obvious threshold to define where in the satellite imagery the "clear" ends and the "clouds" begin. The threshold depends on the problem at hand.

Muench and Keegan[9] approached the problem of determining cloud cover by simply relating observed "opaque" cloud cover to the satellite-observed reflectance, starting with clear conditions and single-layer cloud cover. Data from that study were extended by including some multiple-layer cloud data, to determine thresholds separating "clear," "scattered," "broken," and "overcast" sky conditions. Figure 3 shows the resulting thresholds, in terms of normalized reflectivity* and equivalent IR temperature.**

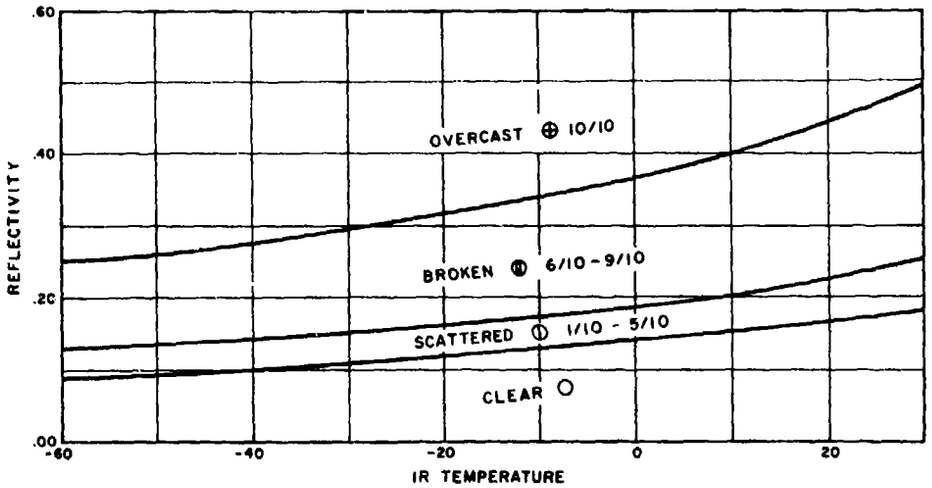

Figure 3. Thresholds Separating Cloud Amount Categories as a Function of Reflectivity and IR Temperature

---

* Normalization corrects for solar geometry and anisotropic scattering.

** Equivalent IR temperature from "Standard IR Calibration," Appendix II, Attachment A3, Corbell, Callahan and Kitsch (1978) The GOES/SMS Users Guide, NOAA/NESS.

9. Muench, H. S. and Keegan, T. J. (1979) Development of Techniques to Specify Cloudiness and Rainfall Rate Using GOES Imagery Data, AFGL-TR-79-0255, ADA084757.

In computing the cloud condition, the model starts with a normalized reflectivity (forecast) R_f and an equivalent IR temperature T_e (degrees C). A parameter B is computed by

$$B = 110R_f / (120 - T_e)$$

and a "minimum" or B_n is computed by

$$B_n = B - 2 \sigma R_f$$

where σ_{Rf} is the standard deviation of reflectivity. The definitions for the cloud categories in terms of B and B_n are shown in Table 2.

Table 2. Definitions of Cloud Amount Categories, Relative to the Parameters "B" and "B_x"

Category	Sky Cover	Limits
Clear	0/10	$0.14 > B$
Scattered	1/10-5/10	$0.20 > B > 0.14$
Broken	6/10-9/10	$0.40 > B > 0.20$ or $B > 0.40$ and $B_n \leq 0.30$
Overcast	10/10	$B > 0.40$ and $B_n > 0.30$

Included in the report by Muench and Keegan[9] is a study of the relation between satellite-observed parameters and surface rainfall. The study was based on widespread precipitation rather than summertime convective precipitation, and should be suitable for use with mid-latitude traveling storm systems. In the study, the relation is presented as isopleths of probability of 0.01 (0.25 mm) of rain the following hour, in terms of normalized reflectivity and IR equivalent temperature.

To parameterize the relation, the reflectivity-IR diagram was first split into two areas by the line

$$R_f = (32 - T_e) / 90$$

The probability of precipitation for one hour PoP_1 can then be approximated by:

for $R_f \leq (32 - T_e) / 90$,

$$PoP_1 = \exp(-11.2\ (1 - R_f)^2)$$

for $R_f > (32 - T_e) / 90$,

$$PoP_1 = \exp(-11.2\ (1 - R_f)^2) \Big/ 1 + \frac{\alpha}{240} + \frac{\alpha^2}{1225}\ )$$

where $\alpha = T_e - 32 - 90R_f$.

The resulting specification of PoP_1 is shown in Figure 4, as a function of R_f and T_e. The isopleths of probability are a fairly good approximation to those

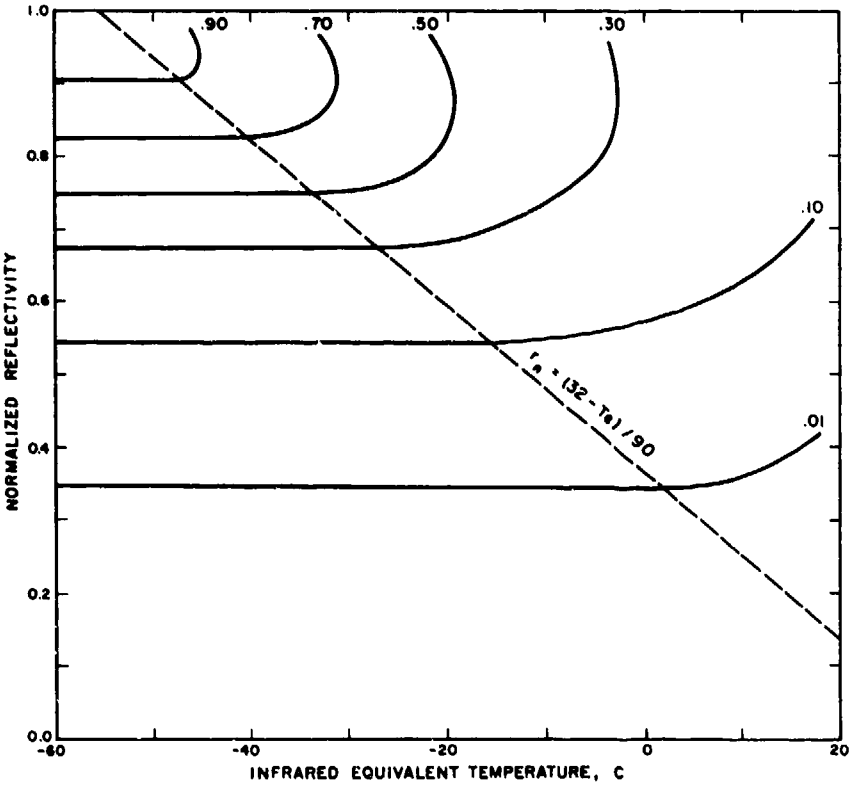

Figure 4. Probability of 0.01 in. of Precipitation the Following Hour, as a Function of Reflectivity and IR Temperature

of Muench and Keegan.[9] The bending of the isopleths toward lower temperature at very high reflectivities does not seem realistic, however, and probably indicates a small underestimate of probabilities in that region.

There are many operational requirements for a vertical resolution of the cloud distribution, particularly for flight planning. An estimate of cloud-top height can be obtained by matching the equivalent IR temperature to some point in the vertical temperature profile. With some other plausible assumptions one could continue and attempt to estimate cloud bases and tops. Consider some limitations, however, if the forecasts are to be verified by ground-based aviation reports. First, the accuracy of estimated cloud heights is no better than about ±20%. Second, when more than one layer is present, the report assigns to the upper layers the sum of the sky coverage up to and including that layer; therefore, cloud amounts of the upper layers are often overestimates in the reports. In view of these limitations, the decision was made to limit this study to only three cloud layers, low (bases below 6500 ft-2000m), middle (bases 6500 ft to 18000 ft--5500 m), and high (bases above 18000 ft). In addition, the forecasts would only be made for the presence or absence of cloud within these layers.

To develop an algorithm for determining presence of low, middle, and high clouds, some 300 simultaneous cloud-observation and satellite measurements were used, from the same data set used for precipitation probability. The cloud layers were plotted on diagrams of reflectivity-versus-IR temperature, and some fairly distinct separations between cloud structures could be seen. For example, warm, bright clouds were low cumuliform clouds, and cold, not-so-bright clouds were cirriform. Figure 5 shows the boundaries for several cloud categories that established the algorithm in the forecast model. Overall, the specifications based on this dependent sample were about 70% correct. Random specifications, however, based on the frequency of occurrence (given some cloud is present) would be about 50% correct.

4. COMPILATION OF TEST DATA

4.1 Satellite Data Source

Since Spring 1977, GOES East Satellite data have been routinely archived at AFGL, using the McIDAS facility. During normal working hours, "1-mile" visible and "4-mile" IR digital values are recorded on magnetic tape for an area from Michigan to Maine, and Quebec to North Carolina (see Section 2 of Muench and Keegan[9] for details). Normally, the imagery data are archived at hourly

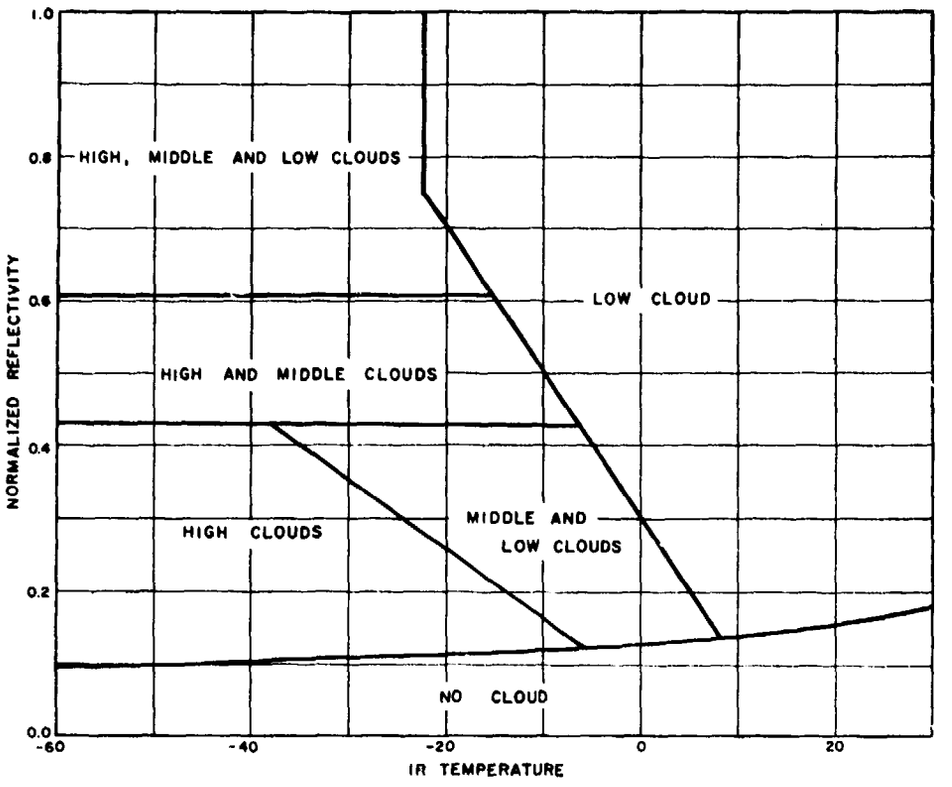

Figure 5. Thresholds of Cloud-Layer Categories as a Function of Reflectivity and IR Temperatures

intervals, which is a little long for objective determination of motion vectors, but on several days during 1978 and 1979 extended periods of half-hourly imagery data were recorded.

Beginning in the Spring of 1980, full disc imagery, with 1/2-mile visible and 4-mile IR data have been recorded routinely on the McIDAS videotape cassettes. To save all cassettes for long time periods would be quite expensive, and a needless duplication of a comparable effort at the University of Wisconsin. So, a 30-day rotating archive is maintained, and each working day two 30-day old cassettes are "written" over and recycled into the file. At any time up to 30 days, one can select an area of interest and times, and extract digital imagery data from the cassettes, exactly as if the data were being received in real time. For the purpose of this forecast test, the rotating archive allowed selection of test cases outside the northeastern United States. Seven fixed areas were set up, similar in size to the standard tape archive. The available storms were such that only three of the areas were used during the fall of 1980. These areas are outlined in Figure 4.

4.2 Upper-Level Winds

As previously explained, a current 700-mb wind was needed, not only as a candidate motion vector, but also to smooth the first objectively determined motion vector of each case. The 700-mb winds were obtained from the 1200 UT 700-mb facsimile chart* for the morning of the case. Winds were obtained from plotted material or reports at three locations within the appropriate area (B, C, or F in Figure 6). The objective motion vectors were computed for the same locations, and the forecast routine used the vector from the nearest of the three locations (e.g., radiosonde stations BUF, ALB, and DIA for area C). In a few instances, the 700-mb wind was either illegible or missing, and either a spatial interpolation was computed, or a geostrophic calculation was made by hand.

4.3 Verification Data

The most extensive data source available for forecast verification is the collection of hourly observations routinely made by airport observers. As part of the satellite archive program, the National Climatic Center has been providing microfische copies of the MF-1-10(A, B) observations forms for 25 of the United States stations shown in area C of Figure 4. The information on this form is more than adequate to verify the forecasts of cloud cover, rainfall probability, and cloud layers. The microfische data were not available for the 1980 forecasts but, since the spring of 1980, the AFGL McIDAS system has been archiving hourly reports received from the high-speed FAA data circuit 604. This weather data archive includes both United States and Canadian airport observations, but is not as complete as the microfische from 10 A, B. Some reports are missed due to communications problems, and the stations report precipitation amount only at 3-hourly intervals, requiring judicious interpolation to verify the hourly precipitation probability forecasts. Also, the reported cloud amounts may include both "opaque" and "thin" clouds, whereas the cloud amount algorithm and the 1979 forecast verification were based only on "opaque" cloud amount.

4.4 Case Selection

The principal application of an extrapolation technique would be to cloud systems that are moving steadily, and pose a threat of rapidly changing weather conditions. Thus, the cases chosen for this test contained cloud patterns associated with traveling cyclone-scale weather systems. Within these cases, orographic clouds are not dominant, if present at all. Cases with extensive convective cloud systems were avoided, as the simple extrapolation model does not include

* Objective plot/analysis prepared by the National Weather Service at the National Meteorological Center

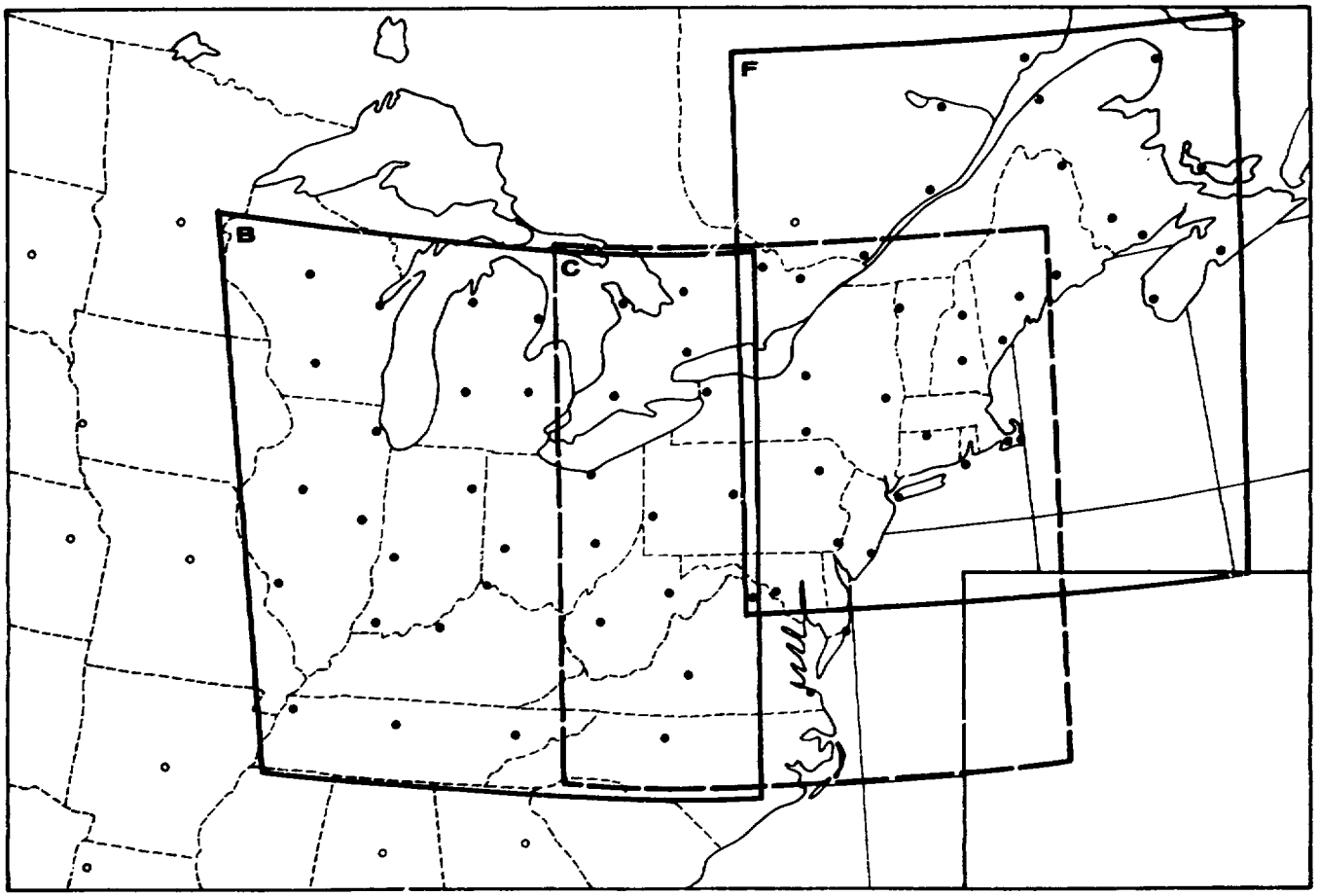

Figure 6. Satellite Data Grid Areas B, C, and F, and Stations Used in Forecast Tests

the effects of the diurnal heating cycle. Also, the model does not have a means to discriminate clouds from snow cover, so, midwinter storms were excluded. Table 3 summarized the cases included in the study. The synoptic weather

Table 3. Cases Used in Weather Forecast Test

Date	Time	Images	Area
14 Nov 1978	1700-2000	6	C
15 Nov 1978	1330-2000	13	C
23 Apr 1979	1700-1800	3	C
24 Apr 1979	1330-1800	10	C
25 Apr 1979	1330-1630	7	C
25 Sep 1979	1330-2000	14	C
2 Oct 1980	1330-1930	13	F, B
17 Oct 1980	1330-1930	13	B
24 Oct 1980	1500-1930	10	B
25 Oct 1980	1400-1630	7	F
3 Nov 1980	1400-1900	11	B
4 Nov 1980	1400-1930	13	C

conditions at 1200 UT for each of the cases are shown in Figures 7a-7l. In general, the cases chosen represent the region ahead of advancing upper-level troughs, characterized by warm-air-advection ("over-running") and extensive, though sometimes patchy, cloud patterns. Systems chosen range from fairly intense storms with moderate to heavy rain, to weak storms with little, if any, rain.

4.5 Satellite Data

Some preprocessing of the satellite imagery data was necessary before the forecast program model was run. First, the forecast stations, which numbered about 25 to 30, were located within the satellite "row-element" coordinate system. A two-stage navigation procedure was used that attains an accuracy of about ±3 NM (5 km).

Next, the visible channel measurements were converted to normalized reflectivity. The 500 x 760 point arrays were split into four sections, and normalization tables were set up for each sector following a procedure described

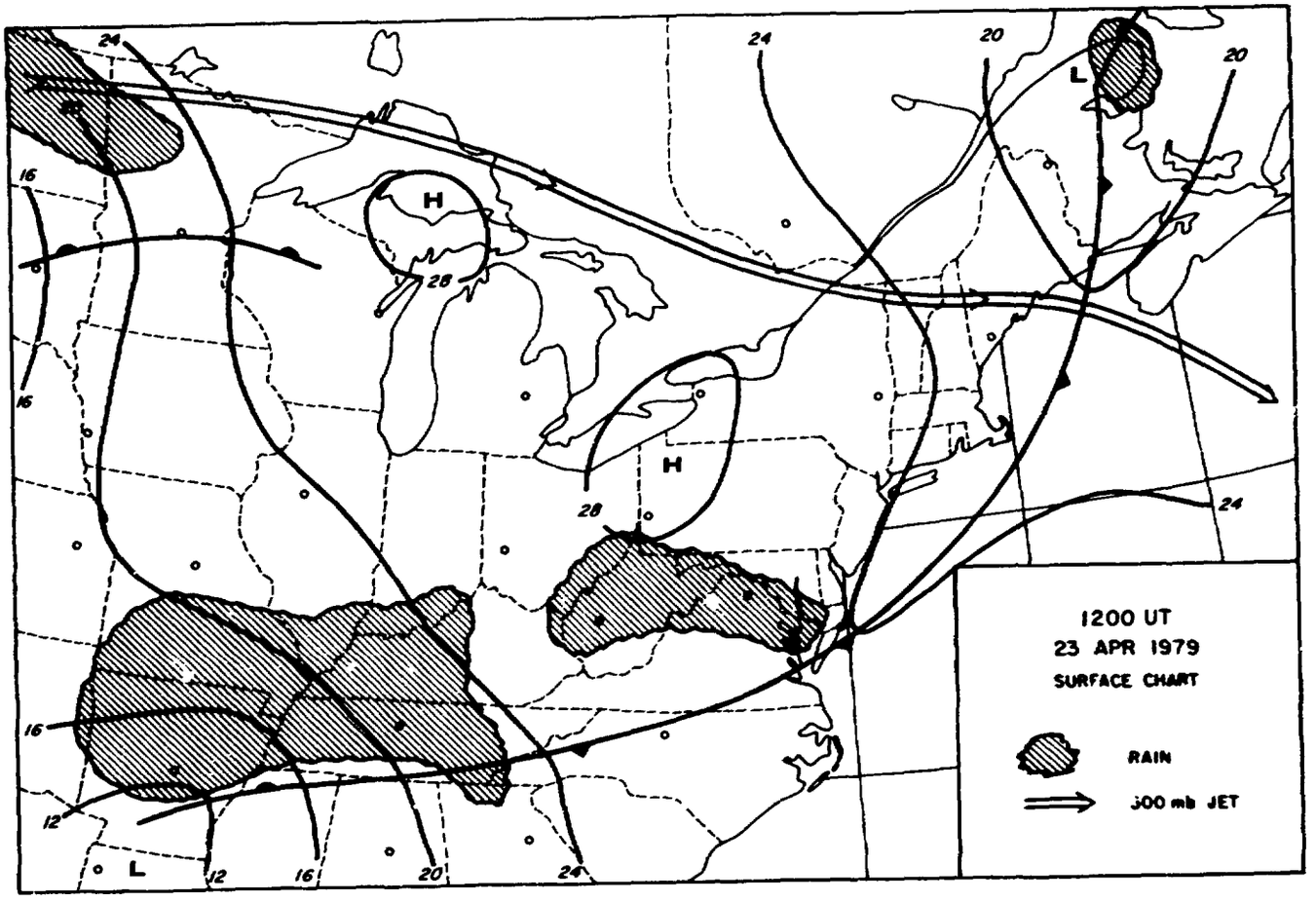

Figure 7a. Synoptic-Scale Weather Conditions for Each Weather Forecast Test Case, 23 Apr 1979

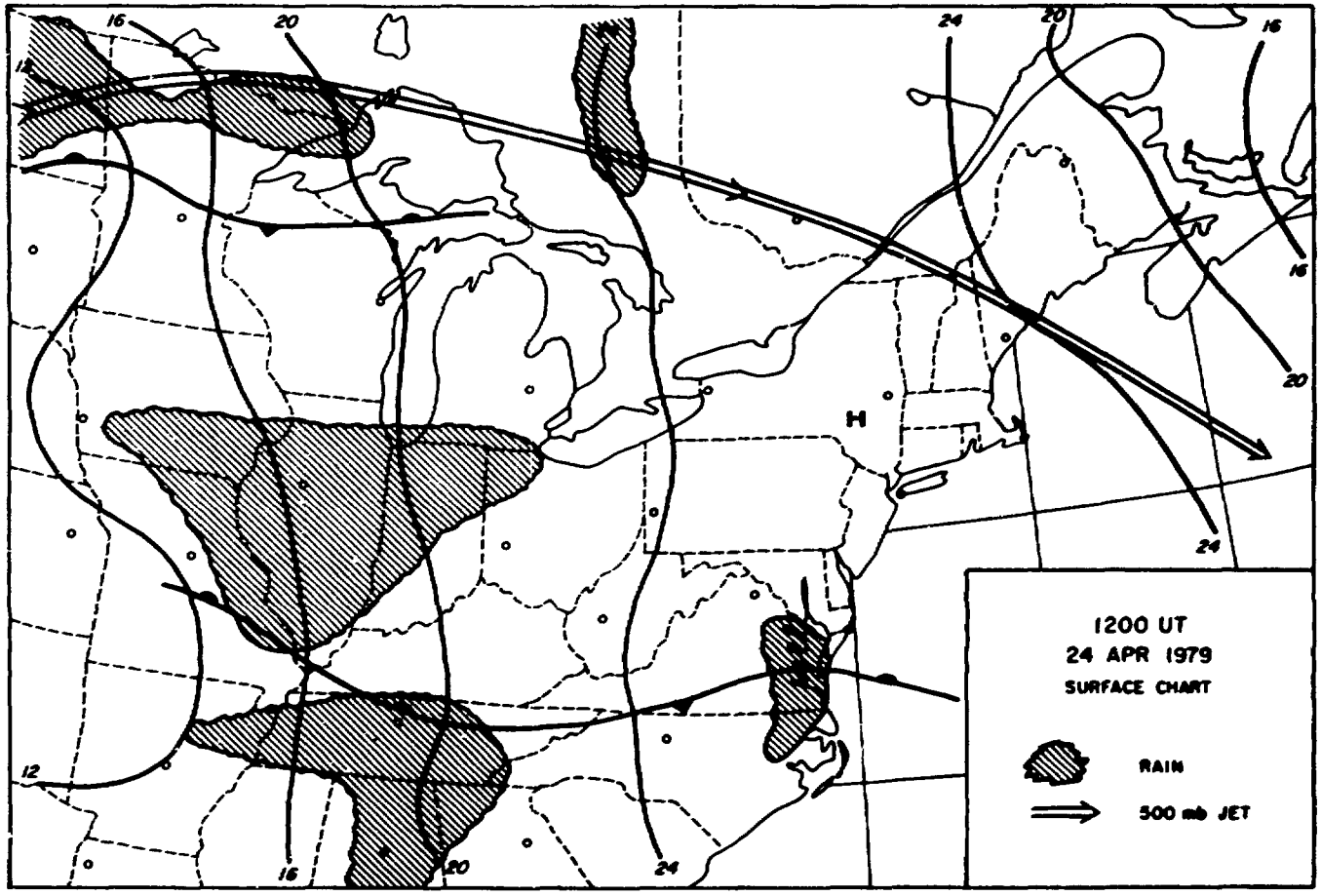

Figure 7b. Synoptic-Scale Weather Conditions for Each Weather Forecast Test Case, 24 Apr 1979

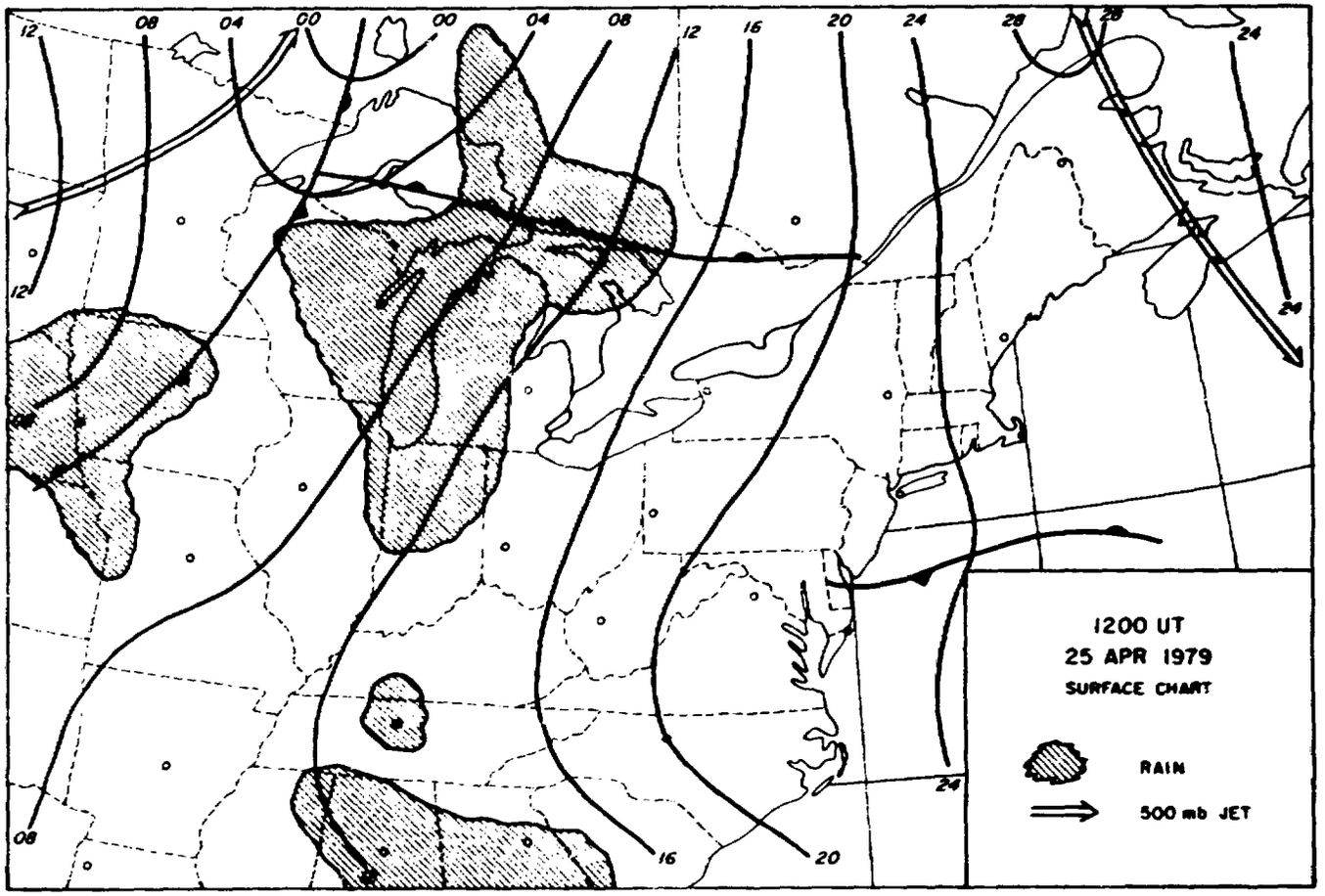

Figure 7c. Synoptic-Scale Weather Conditions for Each Weather Forecast Test Case, 25 Apr 1979

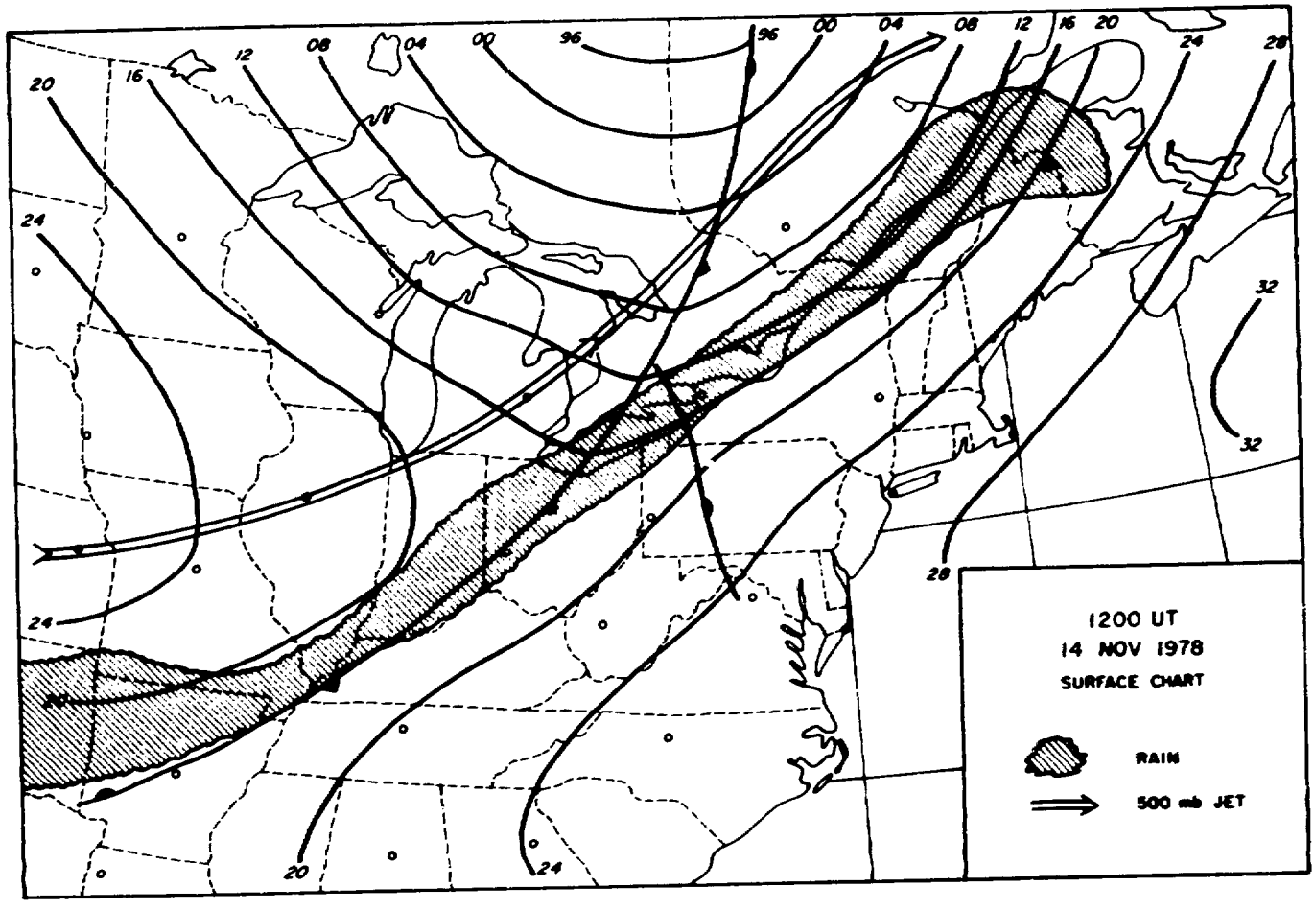

Figure 7d. Synoptic-Scale Weather Conditions for Each Weather Forecast Test Case, 14 Nov 1978

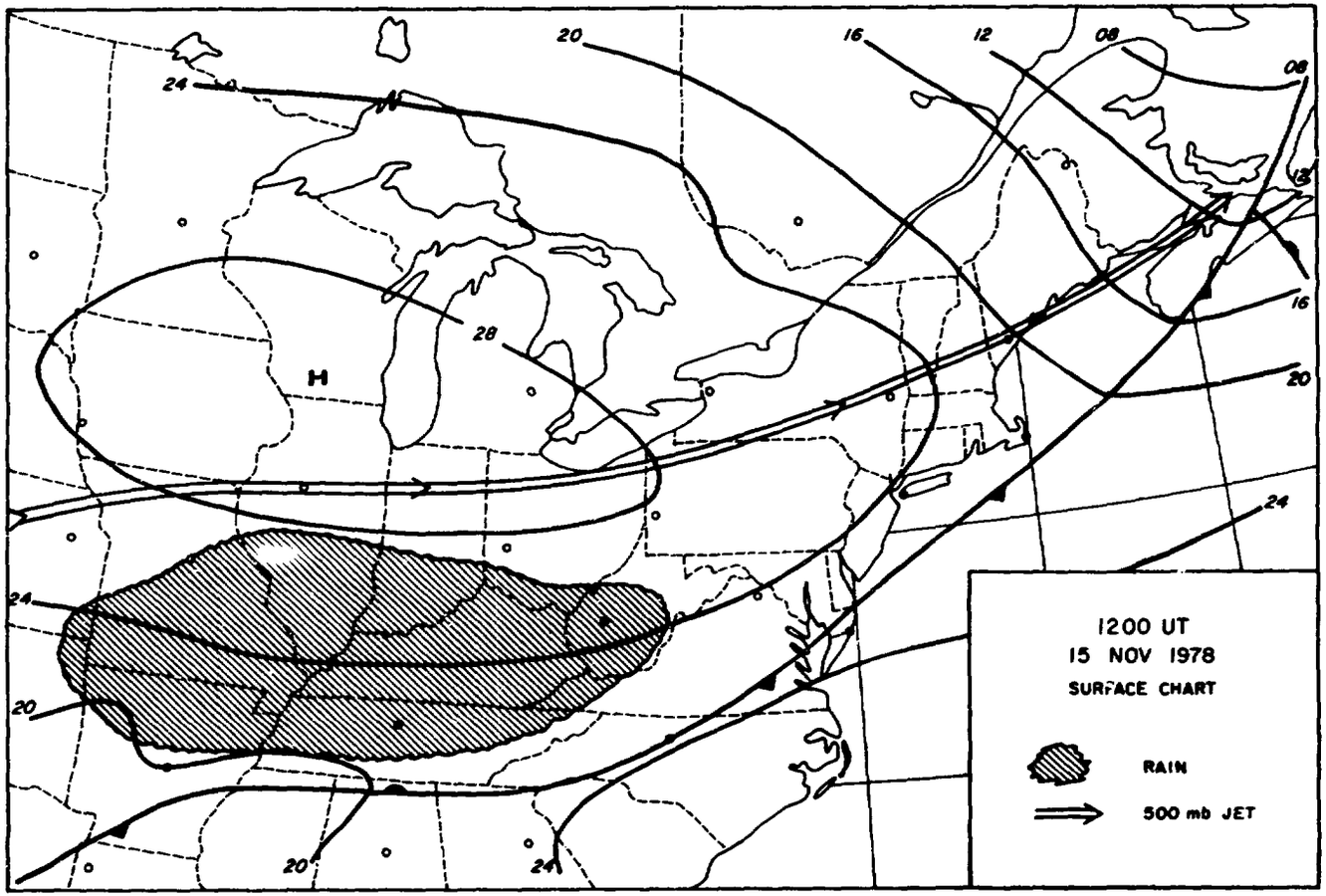

Figure 7e. Synoptic-Scale Weather Conditions for Each Weather Forecast Test Case, 15 Nov 1978

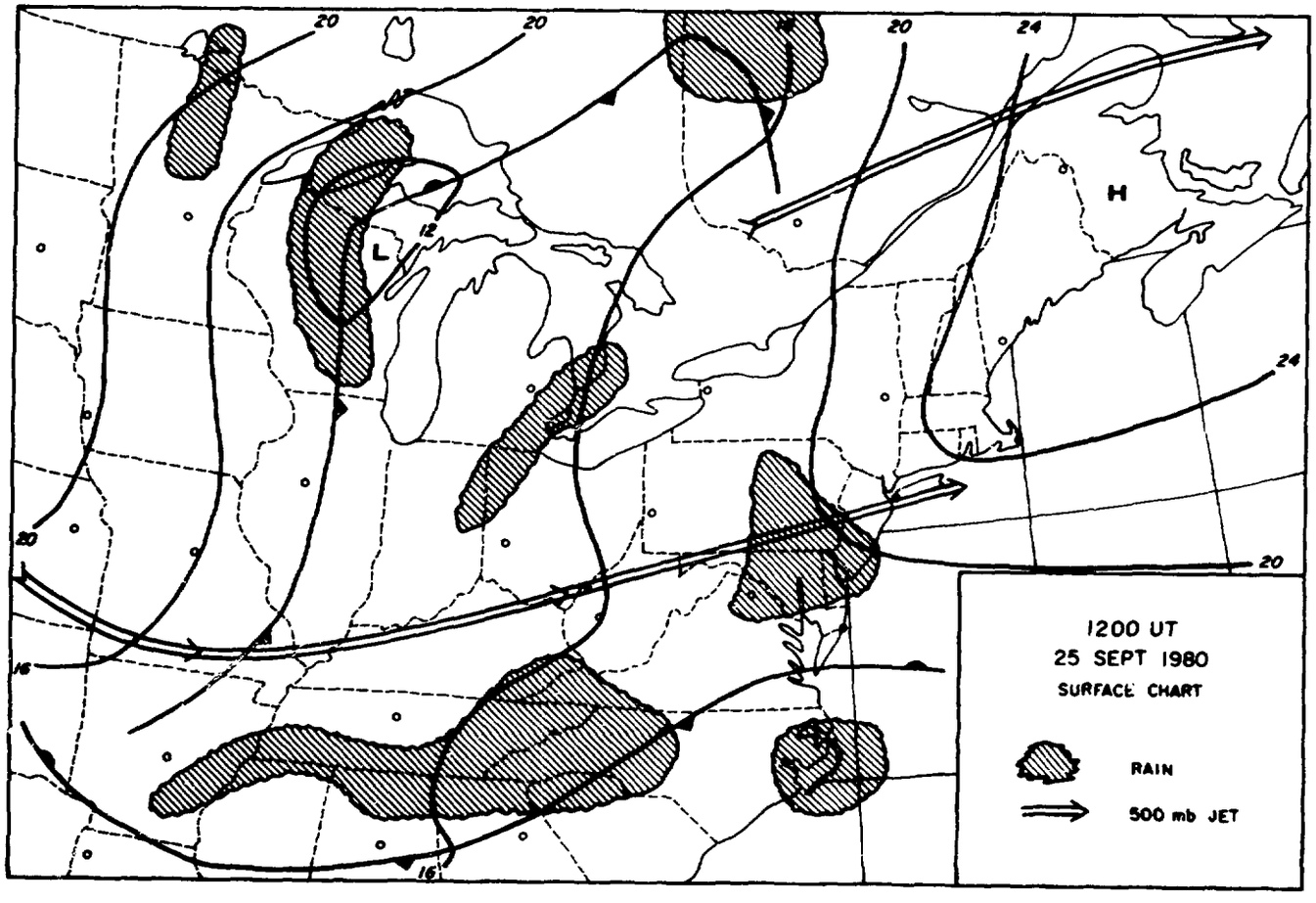

Figure 7f. Synoptic-Scale Weather Conditions for Each Weather Forecast Test Case, 25 Sept 1980

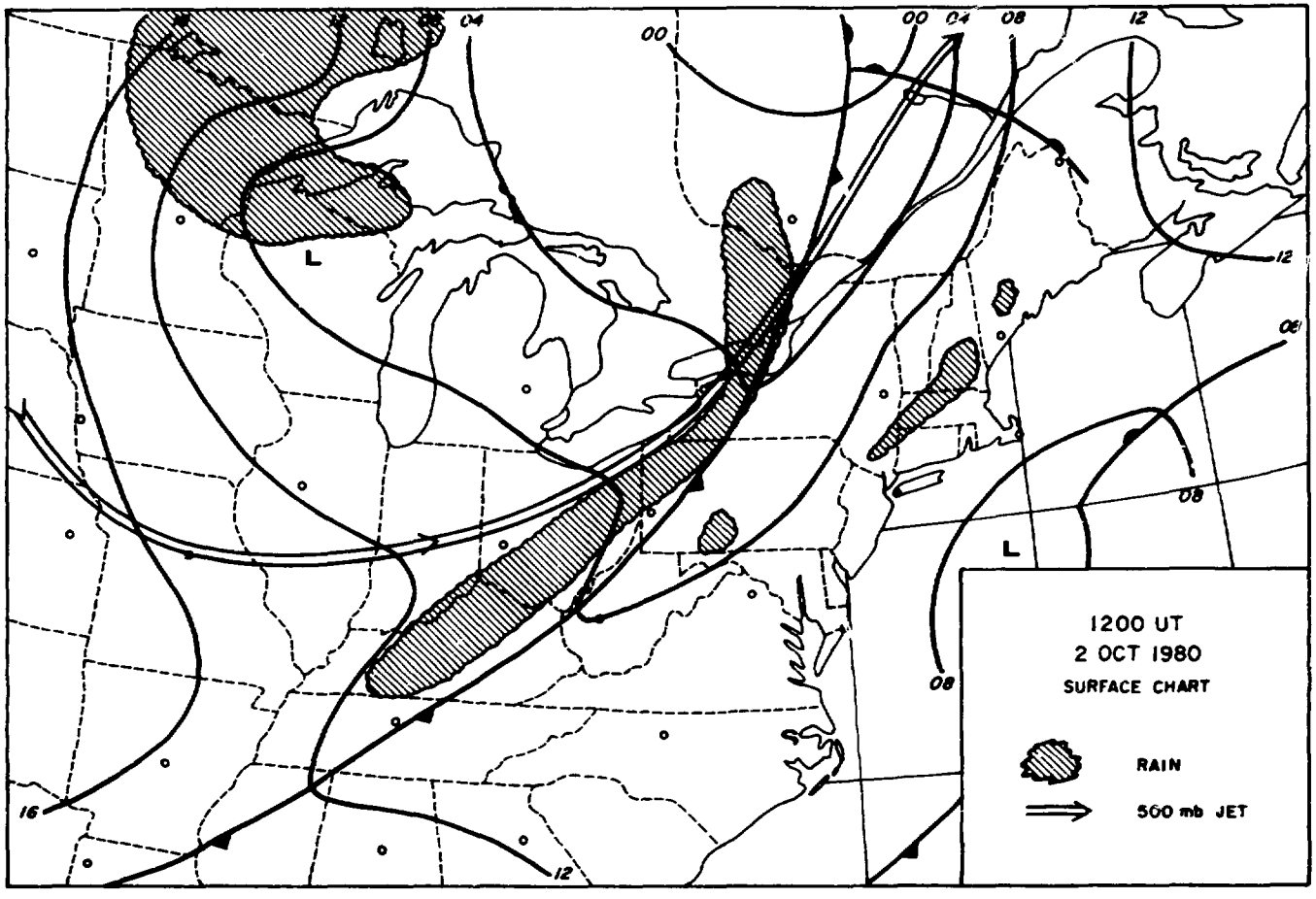

Figure 7g. Synoptic-Scale Weather Conditions for Each Weather Forecast Test Case, 2 Oct 1980

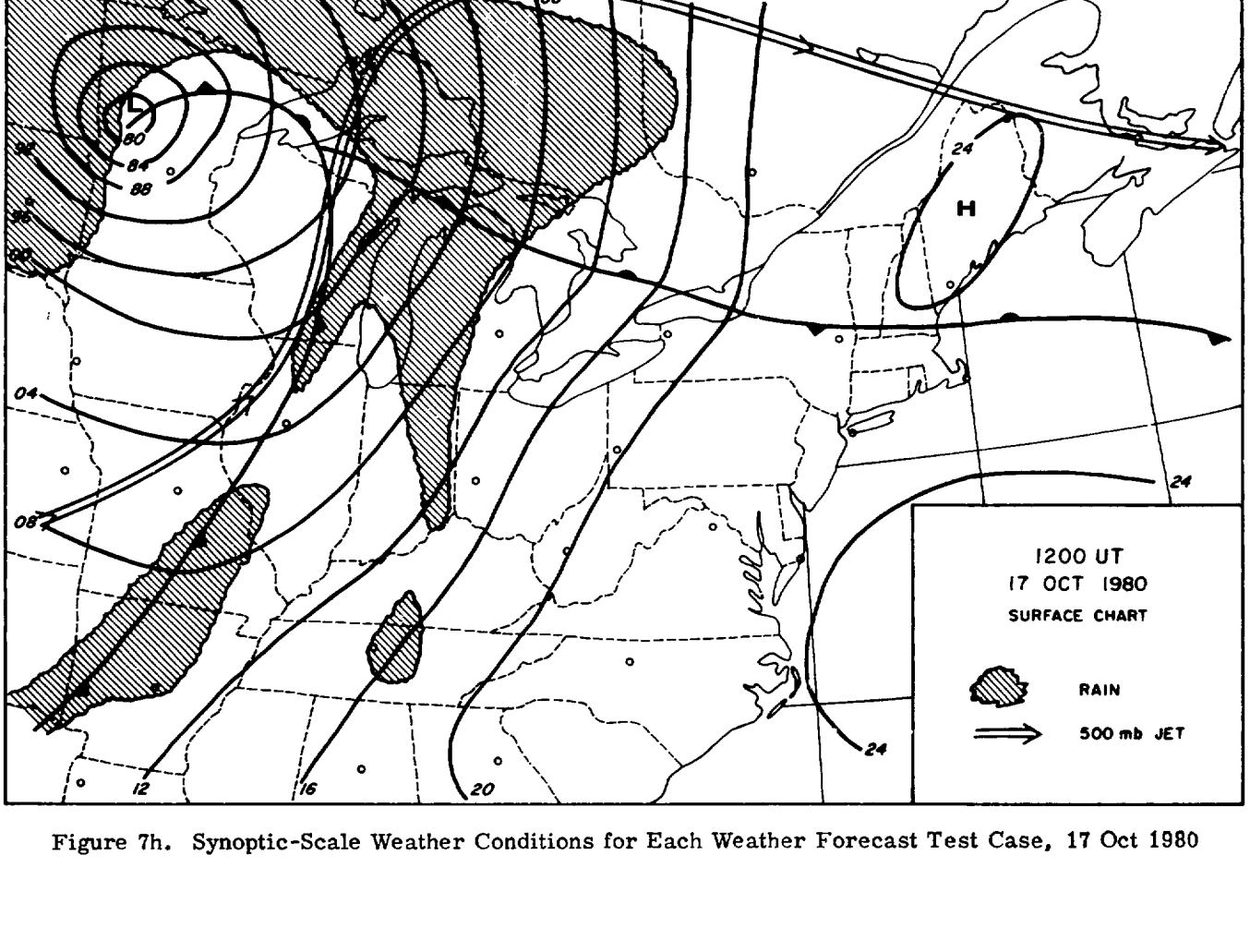

Figure 7h. Synoptic-Scale Weather Conditions for Each Weather Forecast Test Case, 17 Oct 1980

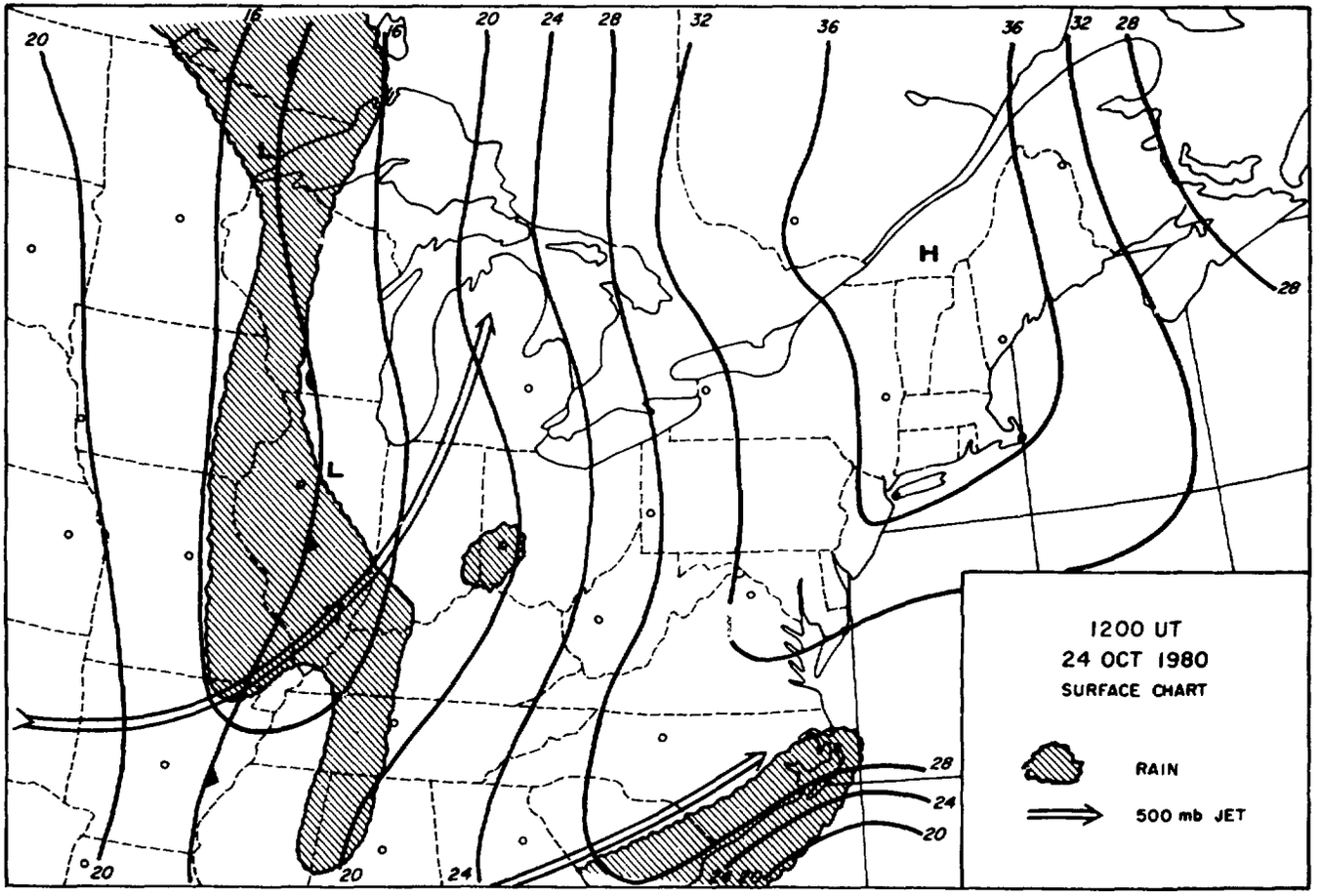

Figure 7i. Synoptic-Scale Weather Conditions for Each Weather Forecast Test Case, 24 Oct 1980

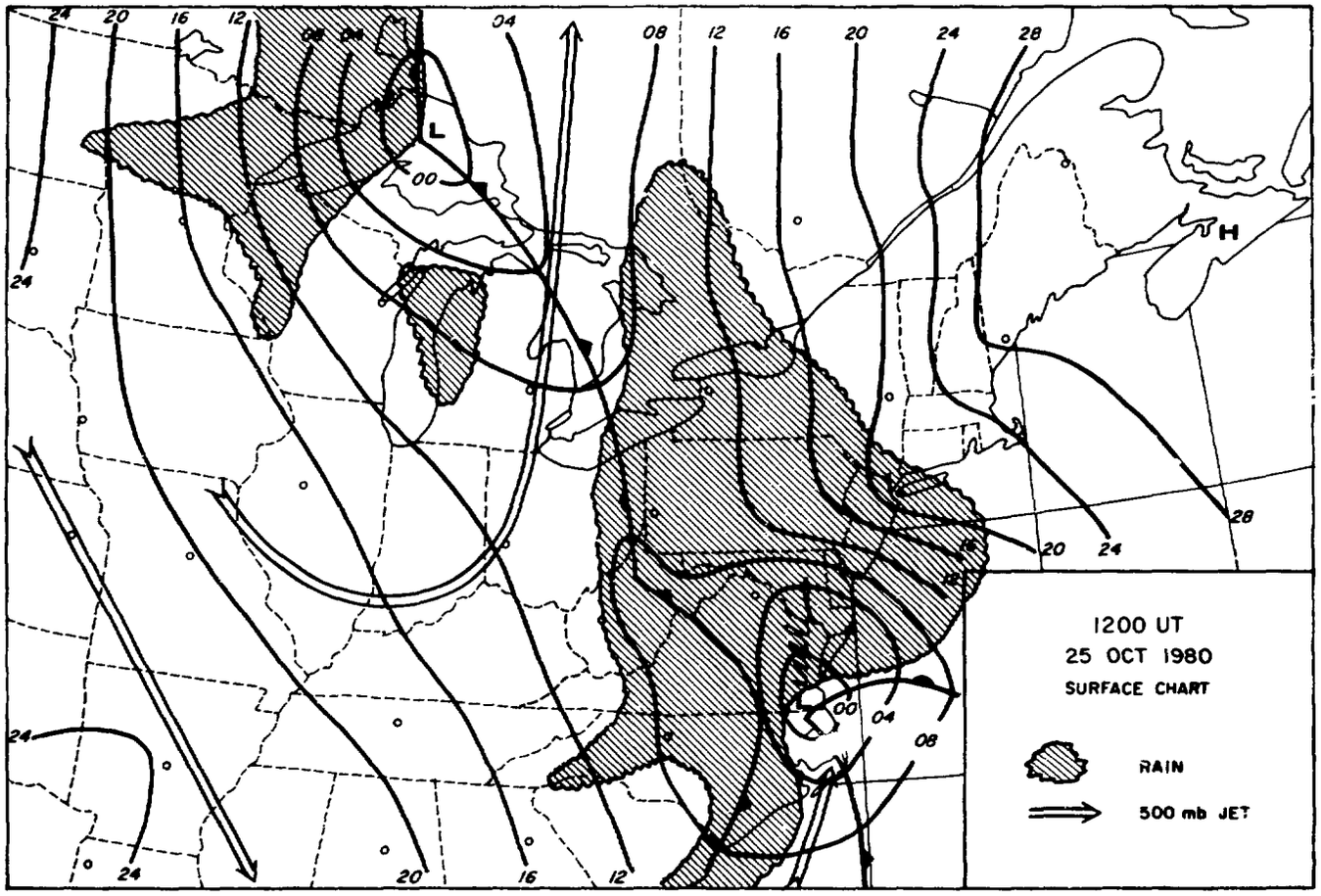

Figure 7j. Synoptic-Scale Weather Conditions for Each Weather Forecast Test Case, 25 Oct 1980

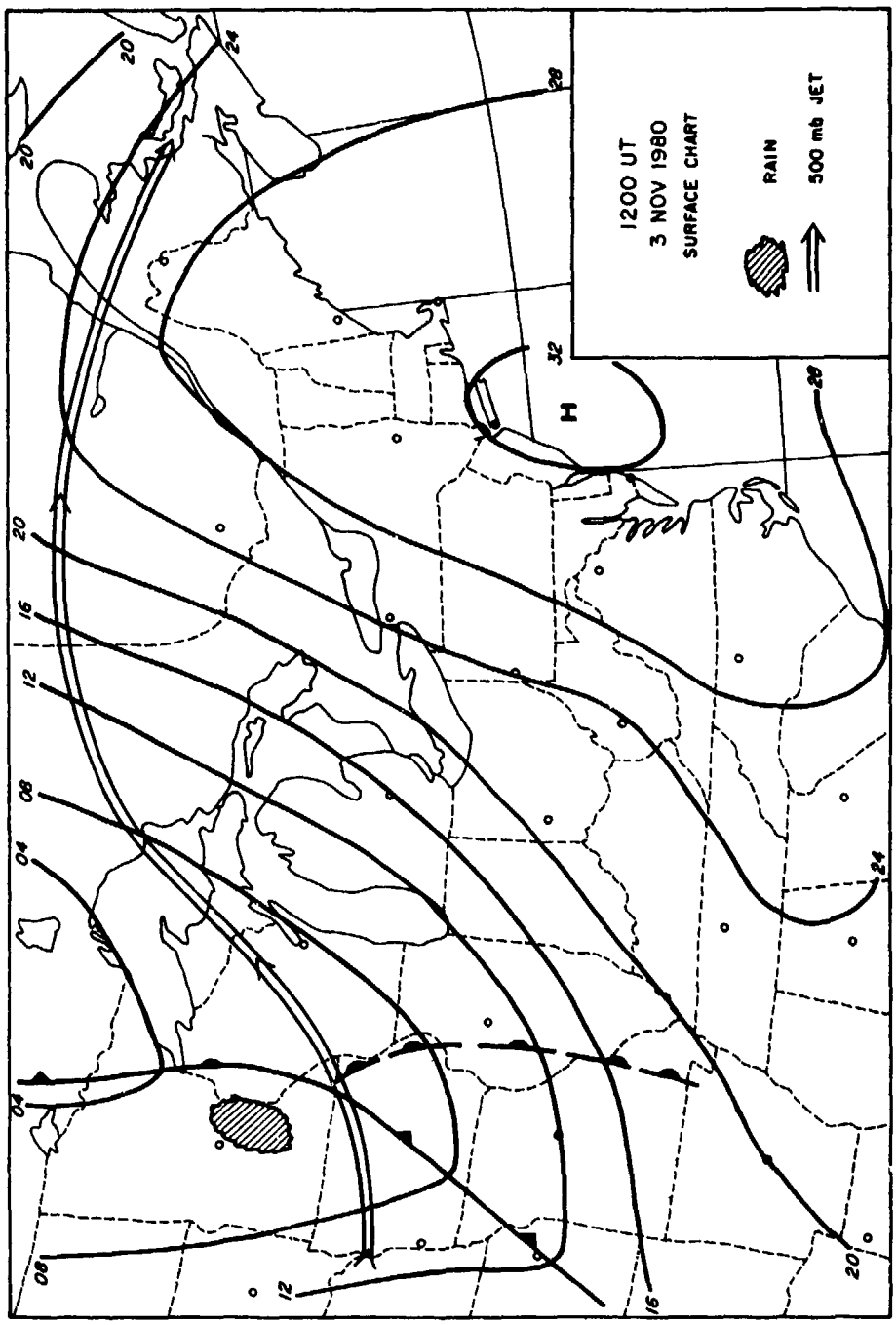

Figure 7k. Synoptic-Scale Weather Conditions for Each Weather Forecast Test Case, 3 Nov 1980

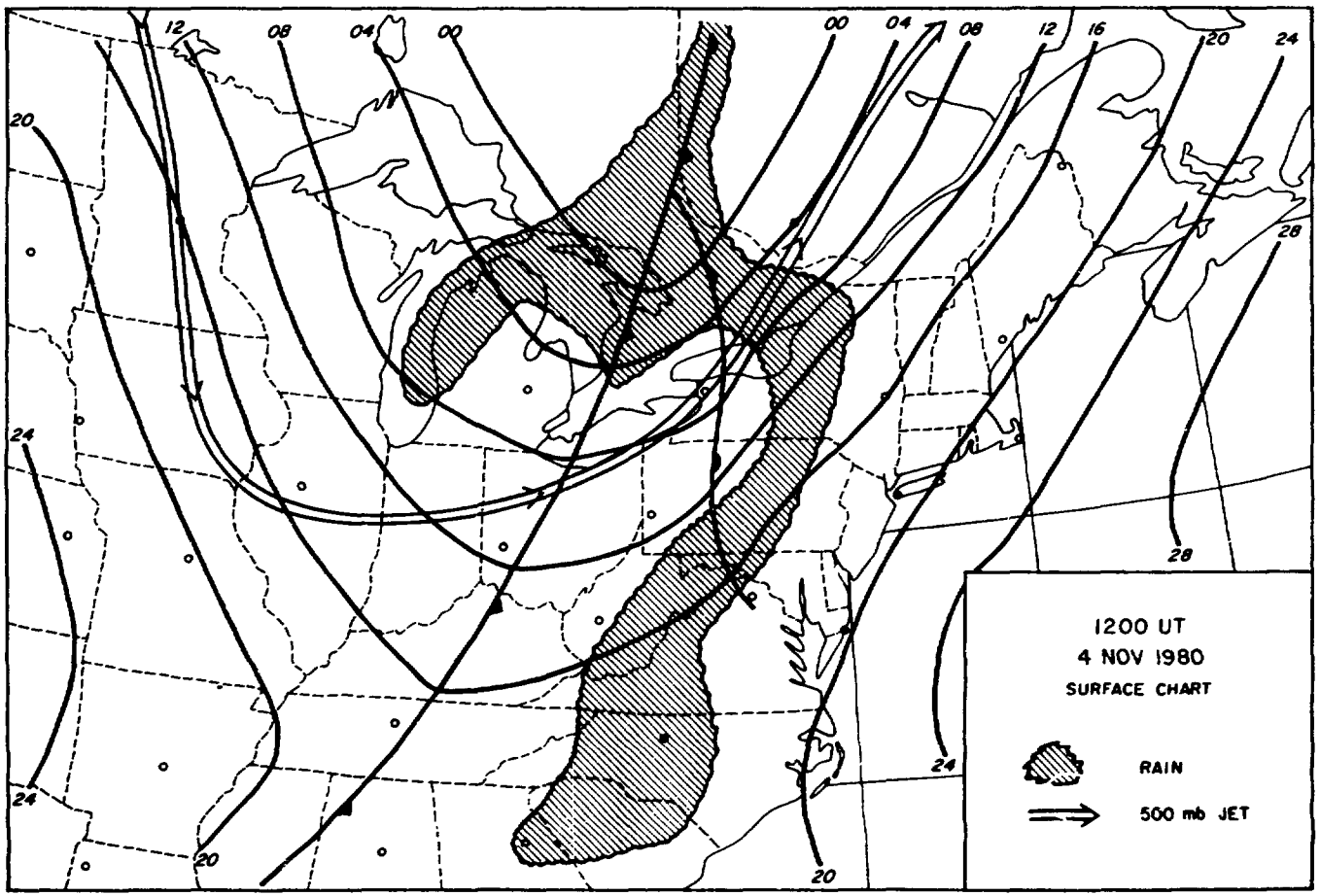

Figure 71. Synoptic-Scale Weather Conditions for Each Weather Forecast Test Case, 4 Nov 1980

in Section 2.3 of Muench and Keegan.[9] The primary factor is the secant of the solar zenith angle. Other factors are the increased reflectivity of layer clouds at low solar-elevation angles, an anisotropic scattering effect, and the small effect of sun-to-earth distance, varying slowly throughout the year. In converting the satellite visible "count" data to reflectance, GOES calibration factors were taken from Tables 5 and 6 of Muench.[10]

The last step in the preprocessing and data extraction was the computing of space-averaged values. This averaging was done to provide consistency in spatial resolution between visible and IR channel values, as well as consistency in spatial resolution between N-S and E-W directions. The N-S resolution of IR channel data was chosen as a standard grid size (about 5.6 NM or 10 km at 40 N). Averages of 4 rows by 7 elements of 1-mile resolution visible reflectivities were computed, as well as averages of one row by 3-1/2 elements of 4-mile resolution IR equivalent temperature. Also, the standard deviation of reflectivity over the 4 x 7 array was calculated. The two spatial averages and the standard deviation for the resulting 106 x 106 array were placed on disc file prior to running the forecast model.

5. FORECAST AND VERIFICATION PROCEDURE

5.1 Forecast Model Execution

The forecast program was executed three times for each test case with its series of consecutive half-hourly imagery data. The separate runs were for the 700-mb motion vector (alone), and for the two runs when motion vectors were computed from the visible and IR imagery using the binary covariance technique. The forecast program, complete with systems routines, used about 62000 (octal) CDC words of storage, and in 120 seconds of CP time would compute forecasts out to seven hours, at 30 stations, for as many as 12 images to a case. For the 700-mb motion vector run, when the binary cross-covariance routine was not used, CP time was cut in half. Examples from the printed output for the case on 25 October 1980 can be seen in Figure 8, including symbols for the weather conditions that were observed. In addition to printed forecasts, there were also forecasts that verified on-the-hour, and were punched onto cards for later verification.

---

10. Muench, H. S. (1981) Calibration of Geosynchronous Satellite Video Sensors, AFGL-TR-81-0050, ADA102894.

Table 4. Verification of Cloud Cover For 4-Hour Forecasts

Visible Ch. Motion Vector

OBSERVED	FORECAST CLR	SCT	BKN	OVC	MSG
CLR	5	10	9	3	3
SCT	23	64	90	42	31
BKN	7	47	104	124	66
OVC	7	17	83	647	170

700-mb Motion Vector

OBSERVED	FORECAST CLR	SCT	BKN	OVC	MSG
CLR	6	8	5	5	10
SCT	25	64	73	47	41
BKN	8	47	100	112	75
OVC	8	20	88	613	191

IR Ch. Motion Vector

OBSERVED	FORECAST CLR	SCT	BKN	OVC	MSG
CLR	5	12	4	3	8
SCT	29	68	68	50	38
BKN	9	45	98	116	82
OVC	11	13	69	612	225

Persistence

OBSERVED	FORECAST CLR	SCT	BKN	OVC	MSG
CLR	8	13	7	3	1
SCT	22	105	67	42	14
BKN	25	95	96	103	29
OVC	13	64	156	649	42

Table 5. Percent Correct for Three Thresholds: 4-Hour Cloud Amount Forecasts

Technique	Clear/Scattered	Scattered/Broken	Broken/Overcast
700-mb M.V.	0.954	0.828	0.773
Visible M.V.	0.954	0.827	0.785
I-R M.V.	0.944	0.833	0.784
Persistence	0.943	0.785	0.740

5.2 Forecast Verification

The two purposes for the forecast test were, first, to determine if the simple extrapolation technique could produce useful short-range forecasts, and, second, to determine which of the three motion vector techniques provided the best forecasts. To judge utility, the best criterion for a short-range forecast is to compare the forecasts to forecasts made assuming "persistence"; in other words, no local change in weather conditions. Forecasters characteristically find only small improvement over persistence with forecasts of less than 12 hours.[11,12] The motion vector technique that scored highest with respect to persistence would, of course, be judged to be the best.

The cloud-amount forecasts were in categories, so the verification program produced 4 x 5 tables of forecast condition versus verification, one set of tables for each time period from 0 to 7 hours. Besides the four forecast categories of clear, scattered, broken, and overcast, there was a "missing" category. For an extrapolation forecast, missing meant the upstream point was outside the data array. For persistence, missing meant the report at the beginning of the forecast period was missing. If the report at the end of the forecast period was missing, there could be no verification. When forecasts are used operationally, the categories are not important in themselves -- a decision is based on whether conditions are expected to be above or below some threshold. The verification program therefore, computed percent correct relative to the three thresholds: clear/scattered, scattered/broken, and broken/overcast.

The same verification procedure was used for the forecasts of the three cloud layers but, in this case, there were only three categories: yes, no, and unknown.

---

11. Hering, W. S. and Quick, D. L. (1974) Hanscom Visibility Forecast Experiments, Proc. AMS Fifth Conf. on Weather Forecasting and Analysis, pp. 224-227.

12. German, K. E. and Hicks, P., Jr. (1980) Air Weather Service Ceiling and Visibility Verification, Proc. AMS Eighth Conf. on Weather Forecasting and Analysis, pp. 339-402.

Table 6. Verification Scores of 4-Hour Forecasts for Cloud Layers

			Visible MV FORECAST			IR MV FORECAST			700mb MV FORECAST			Persistence FORECAST		
			Yes	No	Unk	Yes	No	Unk	Yes	No	Unk	Yes	No	Unk
High	OBSERVED	Yes	280	141	91	266	142	113	263	144	105	306	106	100
		No	100	153	48	106	132	62	97	139	60	64	139	98
		Unk	498	112	133	463	105	178	491	95	152	162	73	508
		Pct. Cor.	0.64			0.62			0.63			0.72		
Middle	OBSERVED	Yes	572	181	145	550	174	181	536	183	172	573	196	129
		No	228	116	67	206	117	92	212	112	86	142	214	55
		Unk	151	36	60	124	43	80	160	26	59	118	23	106
		Pct. Cor.	0.63			0.64			0.62			0.70		
Low	OBSERVED	Yes	673	81	360	616	78	420	631	74	401	862	195	57
		No	174	163	103	169	159	123	157	167	114	74	335	31
		Unk	0	0	2	0	1	1	0	0	2	1	1	0
		Pct. Cor.	0.77			0.76			0.78			0.82		

		1500		1600		1700		1800		1900		2000		2100		2200
YYY	N	CLR	SCT	SCT	SCT	SCT	SCT	SCT	BKN	BKN	BKN	BKN	BKN	OVC	OVC	OVC
	C	NIL	H	H	H	H	H	H	H	H	H	H	H	H	HM	HM
	RP	0	0	0	0	0	0	0	0	0	0	0	0	1	4	14
		●		M		●		●		●		●		●		●
YOW	N	OVC	OVC	OVC	OVC	OVC	OVC	OVC	OVC	OVC	OVC	OVC	OVC	OVC	OVC	OVC
	C	HML	HML	HML	HML	HML	HML	HML	HML	HML	HML	HML	HML	HML	HML	HML
	RP	56	67	62	90	96	98	99	99	99	99	99	97	95	94	96
		●		●		●		●R-		●R-		M		●R		M
YUL	N	OVC	OVC	OVC	OVC	OVC	OVC	OVC	OVC	OVC	OVC	OVC	OVC	OVC	OVC	OVC
	C	HML	HML	HML	HML	HML	HML	HML	HML	HML	HML	HML	HML	HML	HML	HML
	RP	40	52	64	80	93	97	99	99	100	100	100	99	99	97	96
		●		●		●		●		●R-		●R		M		●R-
YQB	N	OVC	OVC	OVC	OVC	OVC	OVC	OVC	OVC	OVC	OVC	OVC	OVC	OVC	OVC	OVC
	C	H	H	HM	HM	HM	HM	HM	HML	HML	HML	HML	HML	HML	HML	HML
	RP	1	1	3	5	8	12	17	24	28	40	57	74	86	93	96
		●		●		●		●		●		●		●		M
YSJ	N	BKN	BKN	BKN	BKN	BKN	OVC	OVC	OVC	OVC	OVC	OVC	OVC	OVC	OVC	OVC
	C	H	H	ML	ML	ML	ML	HM	HM	HM	HML	HML	HML	HML	HML	HML
	RP	0	0	0	0	1	2	3	9	13	19	31	38	44	46	49
		●		●		●		●		●		●		●		●
YCH	N	SCT	SCT	SCT	SCT	SCT	SCT	BKN	BKN	BKN	BKN	OVC	OVC	OVC	OVC	OVC
	C	H	H	H	H	H	H	H	H	ML	ML	ML	HM	HM	HML	HML
	RP	0	0	0	0	0	0	0	0	0	0	1	4	9	19	38
		●		●		●		●		●		●		●		●
YSU	N	CLR	CLR	CLR	SCT	SCT	SCT	SCT	SCT	SCT	SCT	SCT	SCT	SCT	SCT	SCT
	C	NIL	NIL	NIL	H	H	H	H	H	H	H	H	H	H	H	H
	RP	0	0	0	0	0	0	0	0	0	0	0	0	0	0	0
		●		●		●		●		●		●		●		●
ALB	N	OVC	OVC	OVC	OVC	OVC	OVC	OVC	OVC	OVC	OVC	OVC	OVC	OVC	OVC	OVC
	C	HML	HML	HML	HML	HML	HML	HML	HML	HML	HML	HML	HML	HML	HML	HML
	RP	98	96	95	95	95	96	96	98	98	99	100	100	100	99	80
		●R-		●R-		M		●		●R-		●R-		●R-		●R-
PWM	N	OVC	OVC	OVC	OVC	OVC	OVC	OVC	OVC	OVC	OVC	OVC	OVC	OVC	OVC	OVC
	C	HML	HML	HML	HML	HML	HML	HML	HML	HML	HML	HML	HML	HML	HML	HML
	RP	64	47	42	29	23	24	39	48	58	78	85	93	97	100	100
		●		●		●		●		●		●R-		●R-		●R-
AUG	N	OVC	OVC	OVC	OVC	OVC	OVC	OVC	OVC	OVC	OVC	OVC	OVC	OVC	OVC	OVC
	C	HML	HML	HML	HML	HML	HML	HML	HML	HM	HM	HM	HML	HML	HML	HML
	RP	44	43	63	58	53	40	32	20	15	13	15	29	38	50	62
		●		●		●		●		●		●		●R-		●R-
BGR	N	OVC	OVC	OVC	OVC	OVC	OVC	OVC	OVC	OVC	OVC	OVC	OVC	OVC	OVC	OVC
	C	HML	HML	HML	HML	HML	HML	HML	HML	HML	HML	HM	HM	HM	HM	HM
	RP	36	36	35	38	41	53	64	58	44	38	18	9	5	6	10
		●		●		●		●		●		●		●		●

Figure 8. Example of Computed Forecasts from Extrapolation Technique for 25 October 1980, 1500 UT

The unknown category included not only the out-of-array and missing-initial-condition situations, but also the condition when an overcast of middle and high clouds were forecast that precluded an estimate of the low-cloud status. (Note: This area around reflectivity of 0.5 in Figure 5.) When IR temperatures are equally cold, but the reflectivity is much higher, precipitation is highly probable with consequent formation of low clouds. There was also an unknown condition in the verification, representing the layer or layers above an overcast as seen by the ground-based observer. An assumption was made, however, that middle clouds were present whenever rain (but not drizzle) was occurring, and high clouds were present when thunder was heard.

To score the precipitation forecasts, the "P-score" was used.[13] This score is defined by:

$$P = \sum_{i}^{N} \frac{(F_i - O_i)^2}{N}.$$

Where F_i is the forecast probability (0.0 to 1.0) and O_i is the observed condition, either 1.0 or 0.0. The "P-score" represents a mean-square probability error, and the lower the score the better.

6. TEST RESULTS

6.1 Cloud-Cover Forecasts

An example of verification for 4-hour forecasts of cloud amount, an intermediate length forecast, is shown in Table 4. If one compares the numbers, box by box, the numbers, in general, look quite similar; only when looking at the extreme errors does one note that there were many more persistence forecasts of clear and scattered that verified broken and overcast, than for the motion vector extrapolation techniques. The differences show up a little more clearly in the threshold percent correct scores, shown in Table 5.

Some improvement over persistence can be seen at all thresholds for the 4-hour forecasts. This is not the case for all time periods, however, as can be seen in the plots of percent correct, versus time, for each threshold in Figures 9a-9c. At forecast times less than about 2-3 hours, persistence is clearly superior, especially at zero hours. Since the zero-hour forecast is really a

13. Brier, G. (1950) Verification of forecast in terms of probability, Mon. Wea. Rev., 78:1-3.

specification, these results indicate specification accuracy was no better than 0.85 to 0.92 with respect to the thresholds. Since the algorithm was developed on a rather limited data sample, this might be expected. There is also a complication that was overlooked. The "on-the-hour" observations are actually taken 5 to 15 minutes before the hour, while the satellite measurements are made 2-3 minutes (32-33 minutes) after the hour. Thus, there was a 7-18 minute error in the time interval used to compute the motions of the patterns, a factor more important at the shorter forecast times when less horizontal smoothing was used.

In Figures 9a-9c, the forecast scores of the three motion vector techniques are remarkably similar. In fact, none of the three can be said to have a clear advantage for all thresholds and all forecast times.

The curves in Figure 9a would seem to indicate that longer range extrapolations are more accurate than shorter ones, which is contrary to expectations. This actually reflects a bias in the data sample. The algorithm has a problem delineating between clear and scattered conditions, and since the typical case had advancing cloud patterns, the upstream point from clear areas often carried into the cloudy areas for a 7-hour forecast, and the small clear-versus-scattered distinction was not a factor.

There is a very suspicious oscillation in the forecast scores of the extrapolation techniques, with a period of one hour. This oscillation was traced to a systematic difference between forecasts made from on-the-hour satellite data, and on-the-half-hour satellite data. In the case of the former, there were more initial conditions at low solar elevation angles when normalizations are less accurate.

Overall, the cloud amount forecast scores for the extrapolation techniques relative to persistence must be considered as quite encouraging.

6.2 Probability-of-Precipitation Forecasts

The P-scores computed from the four precipitation probability forecast techniques are shown as a function of forecast time in Figure 10. As with the cloud-amount forecasts, we see little difference between the scores for the three types of motion vector. We also see scores worse than persistence for short-term forecasts, and better than persistence for longer forecasts. The crossover for the precipitation forecasts appears between one and two hours, slightly sooner than for the cloud-amount forecasts. This shorter crossover may reflect less observational uncertainty for rainfall, measured by an instrument, than for cloud amount, determined subjectively by an observer. Examination of individual forecasts such as those in Figure 8, suggested there was a systematic over-forecast of precipitation probabilities. This may be due to insufficient compensation for differences

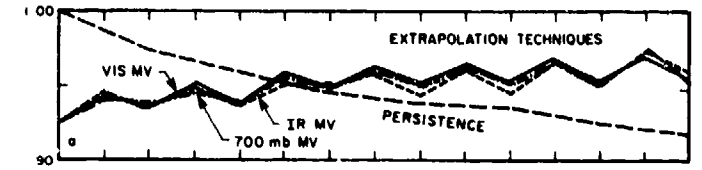

Figure 9a. Percent Correct Scores Relative to Clear-vs-Scattered Threshold, as a Function of Forecast Time

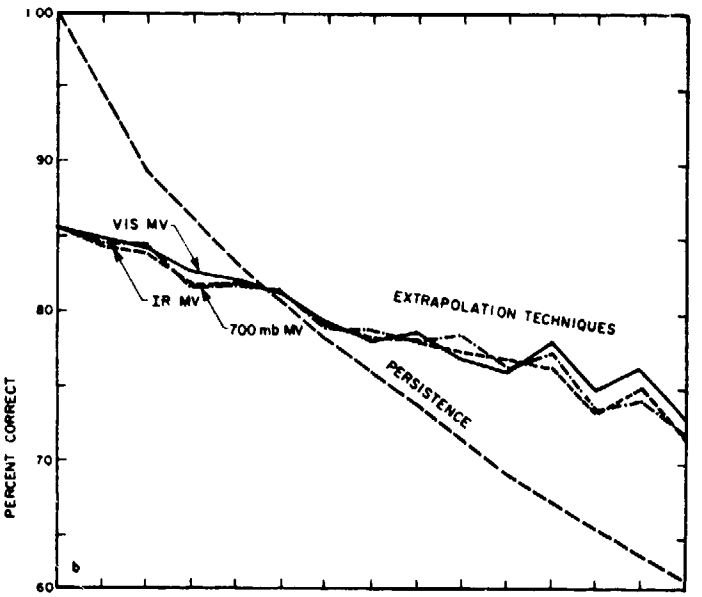

Figure 9b. Percent Correct Scores Relative to Scattered-vs-Broken Threshold, as a Function of Forecast Time

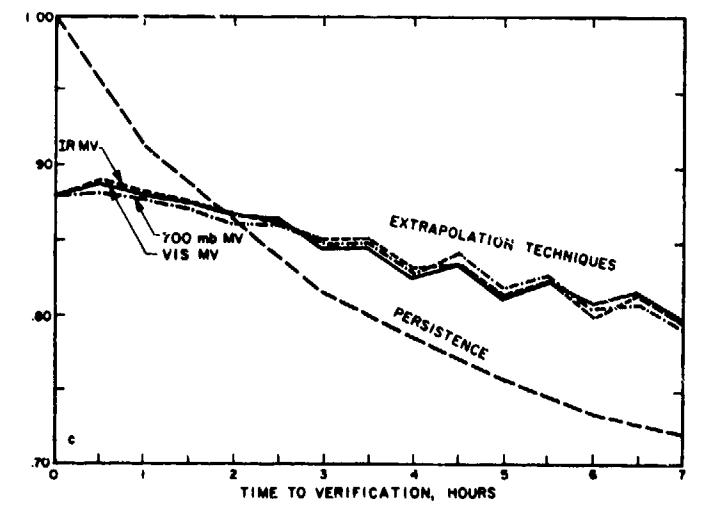

Figure 9c. Percent Correct Scores Relative to Broken-vs-Overcast Threshold, as a Function of Forecast Time

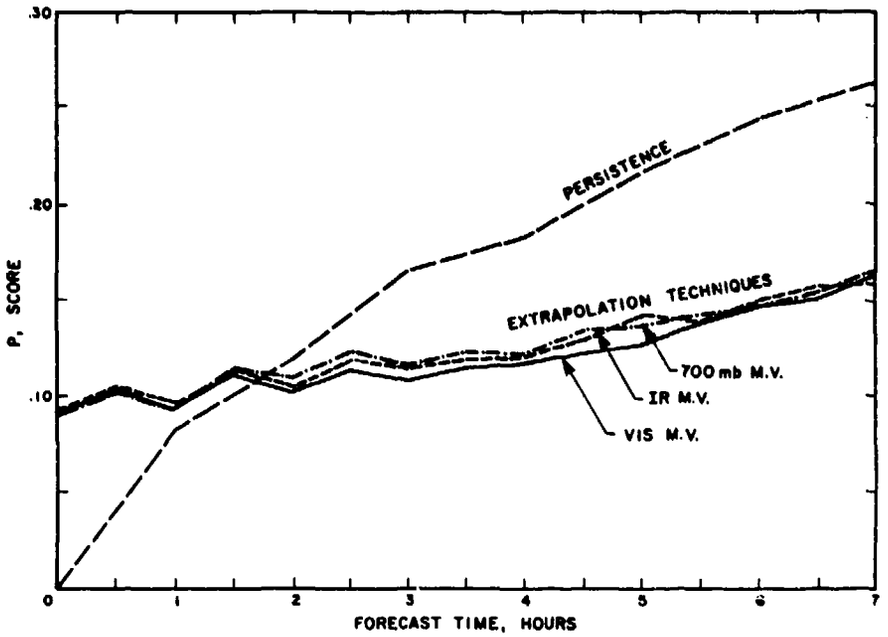

Figure 10. P-Scores of Four Precipitation Probability Forecast Techniques, as a Function of Forecast Time

between the GOES-2 satellite sensors used in the algorithm, and the SMS-2 satellite sensors used in the forecast tests.

6.3 Cloud-Layer Forecasts

An example of verification for 4-hour cloud-layer forecasts is shown in Table 6. One need only look quickly at the percent-correct scores to see that there is no improvement over persistence. The percent correct are plotted against forecast time in Figures 11a-11c for the low, middle, and high cloud layers, respectively. The scores at zero-hours, or specification, were similar to those in the algorithm development sample, and while the specifications are somewhat better than chance, they are obviously worse than persistence for virtually all time periods out to 7 hours. These results are disappointing, and indicate that the combination of motion vector and algorithm did not predict the observed condition as well as did persistence. In the case of cloud layers, "a good observation is the best forecast."

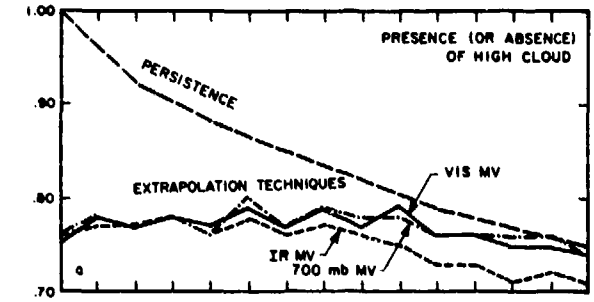

Figure 11a. Percent Correct Scores of Forecast of Low Clouds, as a Function of Forecast Time

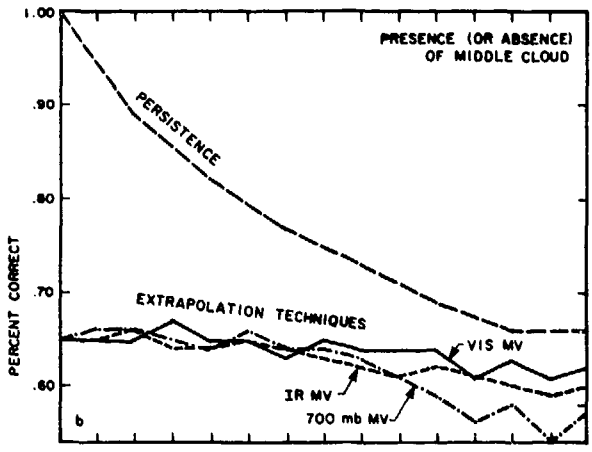

Figure 11b. Percent Correct Scores of Forecasts of Middle Clouds, as a Function of Forecast Time

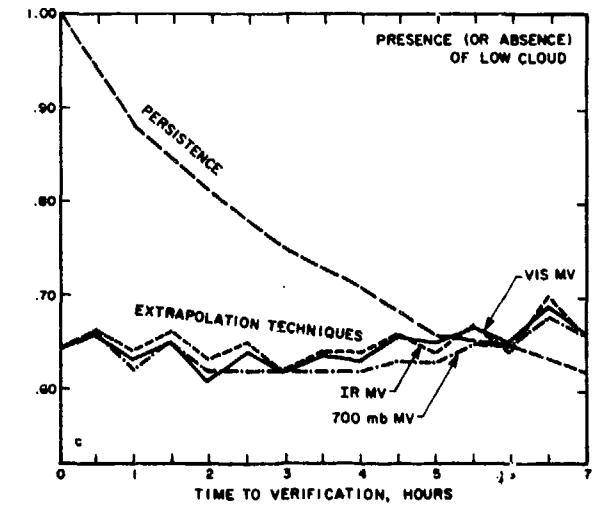

Figure 11c. Percent Correct Scores of Forecasts of High Clouds, as a Function of Forecast Time

7. CONCLUSIONS

Without question, simple extrapolation of satellite imagery patterns can produce useful short-range forecasts of cloud amount and precipitation. In addition, the results shown here can easily be improved upon by using better algorithms[14] and by refinements suggested in follow-up examinations. A note of caution should be added. We still do not know how well a similar extrapolation procedure would have worked, using objective analyses of cloud amount and precipitation fields, rather than the satellite reflectivities and IR temperatures. A study of cloud advection techniques using airways observations and winds aloft was made by Chisholm.[15] While the results are not directly comparable to those presented here, the scores were slightly better than persistence at 3 hours and increasingly better at 6, 9, and 12 hours. Where airways observations are plentiful, the satellite might not add much independent information.

8. FUTURE PLANS

For the near future, we intend to program the simple extrapolation model (initially using 700-mb wind) to use in real-time with the McIDAS facility. With this program, comparisons will be made to subjective forecasts as well as those from NWS model-output-statistics. Extrapolation forecasts of surface-observed cloud and precipitation patterns will also be possible, and such a test would indicate the value of satellites in data-dense areas.

There are obvious limitations to the simple extrapolation model. For example, difficulty should be expected with orographic and convective clouds, and in winter there is the snow-cloud discrimination problem. Thus, efforts will be made to develop more generally applicable models. As a start, work has begun on a two-layer model, with the satellite data being used to estimate condensed water in each layer. The upper layer (about 10,000 ft or 3 km) is presumed to move simply, and can be forecast by extrapolation. The lower layer is presumed to contain a component that also moves simply, as well as a component that is stationary and tied to orographic features. By adopting more appropriate parameters, such as condensed water, one can more easily include other information into the model at a later stage, such as radar reports, or products from fine-mesh numerical models.

14. Keegan, T. J. and Niedzielski, M. (1981) The Specification of Cloud Amounts over Local Areas from GOES Visual Imagery, AFGL-TR-81-0153.

15. Chisholm, D. A. (1962) Cloud and Ceiling Prediction by Advection and by Linear Lag, Travelers Research Center Tech. Memo. 17, 35pp.

References

1. Tarbell, T. C. and Hoke, J. E. (1980) The automated analysis/forecast model system at the Air Force Global Weather Central. Proc. AMS Eighth Conference on Weather Forecasting and Analysis, pp. 262-269.

2. Bellon, A. and Austin, G. L. (1978) The evaluation of two years of real-time operation of a short-term precipitation forecasting procedure (SHARP). J. Appl. Meteor., 17:1778-1787.

3. Leese, J. A. and Novak, C. S. (1971) An automated technique for obtaining cloud motion from geosynchronous satellite data using cross-correlation. J. Appl. Meteor., 10:118-132.

4. Wolfe, D. E., Hall, D. J., and Endlich, R. M. (1977) Experiments in automatic cloud tracking using SMS-GOES data, J. Appl. Meteor., 16:1219-1230.

5. Muench, H. S. and Hawkins, R. S. (1979) Short-Range Forecasting Through Extrapolation of Satellite Imagery Patterns, AFGL-TR-79-0096, ADA073081.

6. Muench, H. S. (1979) Short-Range Forecasting Through Extrapolation of Satellite Imagery Patterns Part II, Testing Motion Vector Techniques, AFGL-TR-79-0294, ADA086862.

7. Muench, H. S. and Lamkin, W. E. (1976) The Use of Digital Radar in Short-Range Forecasting, AFGL-TR-76-0173, ADA033624.

8. Browning, K. A. (1980) Radar as part of an integrated system for measuring and forecasting rain in the UK: progress and plans, Weather, 35, pp. 94-104.

9. Muench, H. S. and Keegan, T. J. (1979) Development of Techniques to Specify Cloudiness and Rainfall Rate Using GOES Imagery Data, AFGL-TR-79-0255, ADA084757.

10. Muench, H. S. (1981) Calibration of Geosynchronous Satellite Video Sensors, AFGL-TR-81-0050, ADA102894.

11. Hering, W. S. and Quick, D. L. (1974) Hanscom Visibility Forecast Experiments, Proc. AMS Fifth Conf. on Weather Forecasting and Analysis, pp. 224-227.

12. German, K. E. and Hicks, P., Jr. (1980) Air Weather Service Ceiling and Visibility Verification, Proc. AMS Eighth Conf. on Weather Forecasting and Analysis, pp. 339-402.

13. Brier, G. (1950) Verification of forecast in terms of probability, Mon. Wea. Rev., 78:1-3.

14. Keegan, T. J. and Niedzielski, M. (1981) The Specification of Cloud Amounts over Local Areas from GOES Visual Imagery, AFGL-TR-81-0153.

15. Chisholm, D. A. (1962) Cloud and Ceiling Prediction by Advection and by Linear Lag, Travelers Research Center Tech. Memo. 17, 35pp.